7732 J. Med. Chem. 2009, 52, 7732–7752
DOI: 10.1021/jm900735p

Journal of Medicinal Chemistry Article

Design, Synthesis, and Examination of Neuron Protective Properties of Alkenylated and Amidated Dehydro-Silybin Derivatives†

Lei Xiang Yang,[‡,§] Ke Xin Huang,[‡] Hai Bo Li,[⊥,§] Jing Xu Gong,[∥] Feng Wang,[§] Yu Bing Feng,[§] Qiao Feng Tao,[§] Yi Hang Wu,[§] Xiao Kun Li,*[,‡] Xiu Mei Wu,[‡] Su Zeng,[§] Shawn Spencer,[⊥] Yu Zhao,*[,‡,§] and Jia Qu[‡]

[‡]*Key Laboratory of Southern Zhejiang TCM R&D, Pharmacy School of Wenzhou Medical College, Wenzhou 325035, China,* [§]*College of Pharmaceutical Sciences, Zhejiang University, Yu Hang Tang Road 388, Hangzhou 310058, China,* [∥]*Shanghai Institute of Materia Medica, Chinese Academy of Sciences, Zu Chong Zhi Road 555, Shanghai 201203, China, and* [⊥]*College of Pharmacy and Pharmaceutical Sciences, Florida A&M University, Tallahassee, Florida 32307*

Received May 28, 2009

A series of C7-*O*- and C20-*O*-amidated 2,3-dehydrosilybin (DHS) derivatives ((±)-**1a**−**f** and (±)-**2**), as well as a set of alkenylated DHS analogues ((±)-**4a**−**f**), were designed and de novo synthesized. A diesteric derivative of DHS ((±)-**3**) and two C23 esterified DHS analogues ((±)-**5a** and (±)-**5b**) were also prepared for comparison. The cell viability of PC12 cells, Fe^{2+} chelation, lipid peroxidation (LPO), free radical scavenging, and xanthine oxidase inhibition models were utilized to evaluate their antioxidative and neuron protective properties. The study revealed that the diether at C7−OH and C20−OH as well as the monoether at C7−OH, which possess aliphatic substituted acetamides, demonstrated more potent LPO inhibition and Fe^{2+} chelation compared to DHS and quercetin. Conversely, the diallyl ether at C7−OH and C20−OH was more potent in protection of PC12 cells against H_2O_2-induced injury than DHS and quercetin. Overall, the more lipophilic alkenylated DHS analogues were better performing neuroprotective agents than the acetamidated derivatives. The results in this study would be beneficial for optimizing the therapeutic potential of lignoflavonoids, especially in neurodegenerative disorders such as Alzheimer's and Parkinson's disease.

Introduction

Neurodegenerative disorders, such as Alzheimer's disease (AD[a]), Parkinson's disease (PD), Huntington's disease, prion disease, and amyotrophic lateral sclerosis, share a common pattern of selective neuronal loss.[1] These devastating ailments are usually accompanied with cognitive and/or motor deficits, affect central nervous system function, and have proved to be incurable, disabling, and even fatal.[2] AD is a typical disorder associated with progressive degeneration of memory and recognition functions of aged people. A definitive hypothesis on the development of AD, which may unify the enormous number of neuropathological and neurochemical findings, has not been established. Although acetylcholine degradation was evidenced to be related to AD syndrome, wherein AChE inhibition continues to be an efficient therapeutic modality for AD treatment,[3,4] increasing studies suggest that excessive reactive oxygen species (ROS) produces oxidative stress and has been implicated in the pathogenesis of neurodegenerative diseases including AD and PD.[5−7]

Clonal pheochromocytoma PC12 cells provide a convenient and well-studied model system for investigation of neuronal injury in vitro.[8] PC12 cells in tissue culture, which possess the ability to be differentiated into neuron-like cells,[9] offer the advantage of combining oxidative stress, mitochondrial function, and cell viability into one model, while the survival of the PC12 cells is reported to be closely related to intracellular ROS scavenging and antioxidant protection of neurons from oxidative damage.[10,11] Moreover, there are growing indications that elevated lipid peroxidation (LPO) is one of the oxidative insults in the pathophysiology of AD[12−14] since studies of cortical tissue from confirmed AD cases have detected increased LPO compared to controls.[15] LPO acts to generate oxygen free radicals within or near membranes, which alter and cleave fatty acid side chains, and cumulative effects of LPO may ultimately destroy membrane integrity and lead to cell lysis. Consequently, inhibition of LPO is tightly associated with the improvement of symptoms in AD patients,[16] and discovery and development of efficient synthetic or natural LPO inhibitors and neuronal protectors are expected to be competent strategies in preventing and treating AD and PD cases. Correspondingly, antioxidants such as vitamins C, E, and certain tested flavonoids, have positive effects in preventing or attenuating these diseases.[17−19]

† This paper is dedicated to MEDI (The Division of Medicinal Chemistry of the American Chemical Society) on the occasion of her Centennial Anniversary celebrations in 2009.

*To whom correspondence should be addressed. For X.K.L.: phone/fax, (86)-571-88208449; E-mail, xiaokunli@163.net. For Y.Z: phone/fax, (86)-571-88208449; E-mail, dryuzhao@126.com.

[a] Aβ, amyloid-β; AChE, acetylcholinesterase; AD, Alzheimer's disease; BQdC, 2,2′-biquinoline-4,4′-dicarboxylate; CD, circular dichroism; DEAD, diethyl azodicarboxylate; DHS, dehydrosilybin; DPPH, 2,2-diphenyl-1-picrylhydrazyl; EDTA-2Na, ethylene diamine tetraacetic acid disodium salt; ERK, extracellular signal-regulated kinase; GPCR, G-protein coupled receptor; LPO, lipid peroxidation; MDA, malondialdehyde; MOMCl, methoxymethyl chloride; MTT, 3-(4,5-dimethylthiazol-2-yl)-2,5-diphenyltetrazolium bromide; NADH, reduced nicotinamide-adenine dinucleotide; NBT, nitroblue tetrazolium; OD, optical density; PD, Parkinson's disease; P-gp, P-glycoprotein; PMS, phenazine methosulfate; PUFA, polyunsaturated fatty acid; ROS, reactive oxygen species; SAR, structure−activity relationship; SD, standard deviation; TBA, thiobarbituric acid; TBARS, thiobarbituric acid-reactive substances; TPP, triphenylphosphine; XO, xanthine oxidase.

 Published on Web 08/12/2009

Chart 1. Structures of Silybin, DHS, and Examples of Modified Silybin Derivatives that are Reported to Possess Moderated Antioxidant Capacity Compared with Silybin.[27,28] [a]

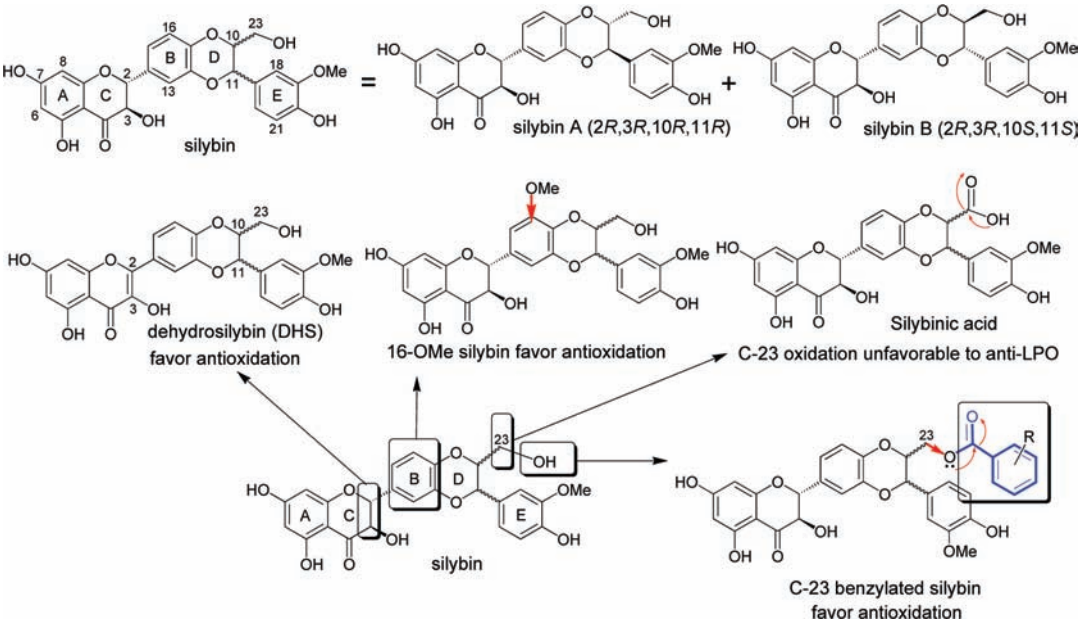

[a] The direction of electron flow is illustrated by arrows.

Silybin (or silibinin) is the major active component of flavonolignans isolated from the seeds of *Silybum marianum* (L.) Gaertner, an Asteraceae plant commonly known as milk thistle. Silybin has been shown to be a member of the large class of flavonoid antioxidants in clinical and experimental tests.[20,21] This lignoflavonoid acts as an important component in Flavobion (Legalon), used clinically as a hepatoprotective drug for several decades.[22] The antioxidant properties of silybin have been intensively investigated and is regarded as a radical scavenger able to reduce liver toxicity from xenobiotics on monooxygenase systems.[23,24] Furthermore, as an antilipoperoxidant, silybin may modulate the fluidity of hepatocyte cell-membranes.[24] Currently, silybin is in clinical trials for the treatment of prostate cancer.[25] Meanwhile, structural modifications of silybin have been carried out with a focus on elevating the aqueous solubility of silybin analogues to facilitate in vivo hepatoprotective use. In a prodrug approach, the oleate, palmitate, and phosphate at C7−OH of silybin as well as the C20−OH phosphate of silybin have been prepared as pro-forms, making the derivatives more lipophilic or hydrophilic;[26] however, pharmacological descriptions were missing in literature reports. Additionally, two tetra-acetoxyl derivatives were synthesized at all of the C3−, 5−, 7−, and 20−OH positions of silybin, but their biological activities were not indicated.[22]

In our ongoing research investigating flavonolignan analogues, various substituents were introduced into the B- and E-ring of silybin. The analogue owning a methoxy group in the B-ring exhibited apparently improved superoxide anion free radical scavenging (Chart 1), even better than quercetin, one of the most potent flavonoid antioxidants.[27] In addition, a series of regiospecific C23 esterified silybin analogues were prepared, most of which exhibited more effective anti-LPO activities and/or better protective capacity against H_2O_2-induced DNA damage than silybin (Chart 1).[28] This indicated that rational design and preparation of silybin derivatives may enrich the knowledge base of antioxidant and neuroprotective lignoflavonoids.

2,3-Dehydrosilybin (DHS), a natural silybin derivative responsible for the yellow color of silymarin complex, is present in the *Silybum* species at rather low levels.[22,29] Unlike silybin, the biological investigations on DHS are limited, partially due to its low yield and poor water solubility (i.e., lower than silybin). A recent report, however, indicates that DHS demonstrates significantly greater antioxidant activity over silybin.[22] Cell-level experiments reveal that pretreatment with DHS may effectively protect human keratinocytes and mouse fibroblasts suffering from H_2O_2-induced damage, thus enhancing the repair and healing process in cutaneous tissue.[30] Additional investigations reveal that DHS promotes cell protection against H_2O_2-induced HepG2 cell death and also shows superior protection against galactosamine-induced liver injury in vivo in comparison to silybin.[31] Very recently, DHS was subjected to an assay of DNA topoisomerase inhibition and proved to be a better topoisomerase inhibitor than the parent silybin.[32] As a result, structural modification and intensive pharmacological studies on DHS are essential. Nonetheless, only several reports are currently linked to studies on DHS analogues. Some studies incorporating methylation on C3−OH, C7−OH, and C20−OH, as well as benzylation on C7−OH, were accomplished[33] and the derivatives exhibited effective P-gp inhibitory activity.[34] Moreover, the C23 hydroxymethyl when oxidized to a carboxyl group (i.e., silybinic acid) unexpectedly results in reduced solubility, poor radical scavenging and antioxidant potential, and does not readily conform to flow cytometry assays for evaluating P-gp activity (Chart 1).[22,34] Alkenylation of DHS directly on the A-ring carbon skeleton affords prenylated and geranylated DHS analogues, while the geranylated derivatives provide better affinity to P-gp than the prenylated analogues.[35] Comparatively, prenylation at C8 exhibits better P-gp affinity compared to C6 prenylation of DHS.[35] Recently, a series of multiphenylated and some dimeric DHS derivatives were prepared to analyze the free radical scavenging mechanism of these DHS analogues.[36]

Scheme 1. Synthesis of (±)-Silybin and (±)-Isosilybin[a]

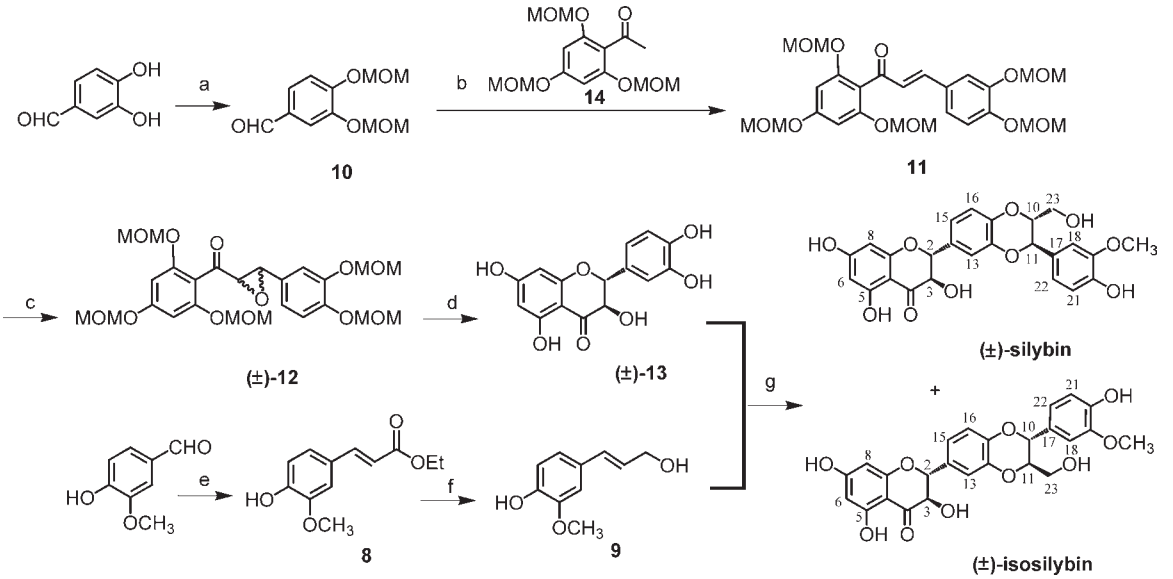

[a] Reagents and conditions: (a) MOMCl, NaOH, Bu_4NBr, $CH_2Cl_2-H_2O$, rt, 4 h; (b) **14**, KOH, MeOH, rt, 10 h; (c) H_2O_2, NaOH, MeOH, rt, 5 h; (d) HCl, MeOH, 55 °C; 2 h; (e) $Ph_3P = CHCO_2Et$, $CHCl_3$, reflux; (f) $LiAlH_4-AlCl_3$, dry THF, rt, 1 h; (g) Ag_2CO_3, dry benzene−acetone, 55−60 °C, 20 h.

Although there are more than 1500 research papers related to silybin or silymarin, the vast majority address radical scavenging, hepatoprotective, and anticarcinomic properties while reports on neuroprotective properties are still insufficient. Among the currently limited number of investigations concerning neurotropic and neuroprotective properties of silybin, the finding of microglia activation on BV-2 cells indicates that silymarin may not only inhibit lipopolysaccaride-induced neurotoxicity in mesencephalic mixed neuroglia cultures but also reduce damage to dopaminergic neurons.[37] Additionally, two independent research groups employed PC12 cells to evaluate antioxidant prevention of apoptosis following nerve growth-factor withdrawal[38] and protection against L-glutamate induced neurotoxicity, respectively.[39] Silymarin complex is believed to provide some protection to primary hippocampal neurons from oxidative stress-induced apoptosis.[38] However, silymarin is reportedly unable to protect PC12 cells from L-glutamate-induced cell death.[39] Other investigators observed rat brain protection from drug-induced oxidative stress and decreased LPO in rat cerebral tissue following treatment with standardized silymarin extract.[40] The only known studies on human neuroblastoma cell lines (NB-1 and IMR32 cells) report silymarin effects on neuro-immunomodulation.[41] More evidence is needed to identify the neuroprotective properties of silybin and DHS as well as their analogues. This stimulated our interest to pursue neuroactive and neuroprotective effects owing to the molecules. No systematic investigations on C7−OH and C20−OH substituted analogues of silybin and DHS for their antioxidant and neuroprotective effects have been clearly performed. Furthermore, the nitrogen atom (which plays an important role in AChE inhibitors) has not been mentioned in reports to date about silybin-derived lignoflavonoids, especially with regard to neuronal cell protective characteristics.

Amide functionality plays an important role in a variety of bioactivities. Numerous compounds exhibit increased bioactivities upon introducing an amide moiety into the molecules. For example, adding of a salubrinal analogue into the biotin molecule enhances the protective ability of PC12 cells against apoptosis induced by endoplasmic reticulum stress.[42] Some designed dipeptides are also known to be potent LPO inhibitors,[43] as bringing in a lactam moiety assists dimerumic acid at inhibiting LPO efficiently even in low concentrations.[44] Furthermore, the nitrogen-bearing quinazoline and its derivatives efficiently reduce aggregation of mutant Huntington protein, which alleviates toxicity to PC12 cells.[45] It is thus suggestive that employing an amide may well enhance the chelating capacity of molecules to Fe^{2+},[46] beneficial in LPO inhibition and the treatment of AD.[47]

Directing an alkenyl moiety into flavonoid-based molecules may be an efficacious strategy of improving cytoprotective effects of the molecules,[48] as either linear or branched alkenyl chains in flavonoids reportedly antagonize LPO.[48,49] The synergistic effect of allyl groups is likely attributable to its electron-deficiency, and inserting this moiety into molecules can also elevate scavenging ability of superoxide anions.[50] Moreover, the oxidant mediator of low-density lipoproteins (15-lipoxygenase) is believed to be inhibited more effectively by a benzene derivative possessing an *O*-allyl group[51] and is correlated with inhibition of LPO and protection of PC12 cells.

A survey of current results suggests that DHS derivatives possessing amide and alkenyl functional groups should be incorporated into our ongoing SAR study. These lipophilic alkenyl groups are considered more prone to increase the molecule's ability to penetrate membranes, which would facilitate the molecules' passage through the blood−brain barrier of AD and PD patients.[52,53] In addition, the reactive amide oxygen may participate in complexation of Fe^{2+}, which is conducive to inhibiting LPO and protecting brain tissue from the AD process.[47] The variant electron density and heteroatom attributable to amide substituents may not only form more $\sigma-\pi$ or $\pi-\pi$ and inter- or intramolecular hydrogen bonds but also provide the designed analogues more opportunity to form binding sites with specific neighboring protein domains of metabolic enzymes in neuronal cells or brain tissues.

Scheme 2. Synthesis of Dehydro-Silybin Derivatives (±)-**1**−(±)-**5**[a]

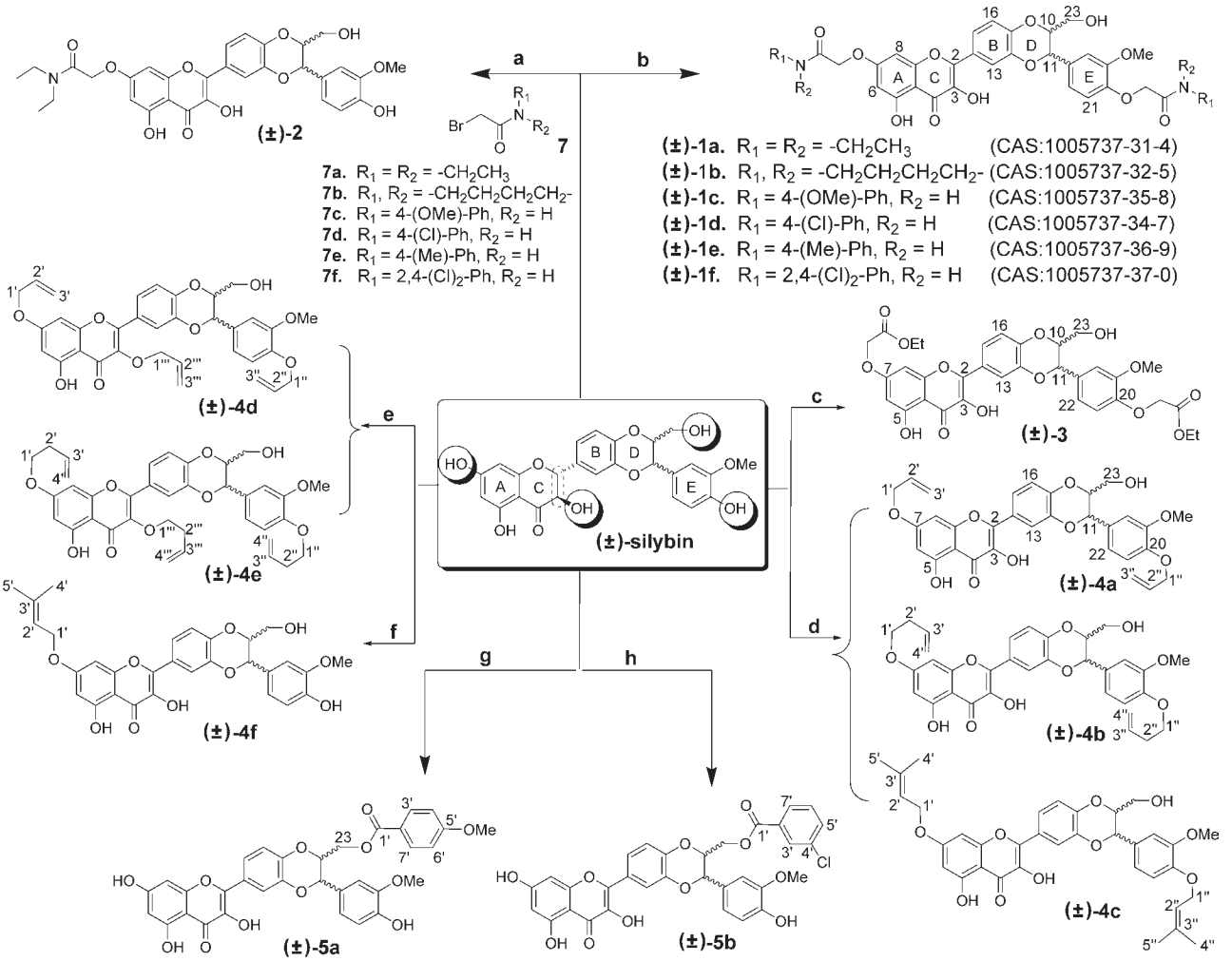

[a] Reagents and conditions: (a) K_2CO_3, KI (cat.), DMF, 1.0 equiv of **7a**, 45 °C, 12 h; (b) K_2CO_3, KI (cat.), DMF, 2.2 equiv of **7**, 45 °C, 12 h; (c) $ClCH_2CO_2Et$, K_2CO_3, KI (cat.), DMF, 45 °C, 12 h; (d) 2.2 equiv of allyl bromide (for **4a**)/butenyl bromide (for **4b**)/isopentenyl bromide (for **4c**), K_2CO_3, DMF, 55−75 °C, 2−3 h; (e) 3.3 equiv of allyl bromide (for **4d**)/butenyl bromide (for **4e**), K_2CO_3, DMF, 75 °C, 3 h; (f) 1.0 equiv of isopentenyl bromide, K_2CO_3, DMF, 55 °C, 1 h; (g) 4-MeO-benzoic acid, TPP, DEAD, THF, 60 °C, 10 h; (h) 3-Cl-benzoic acid, TPP, DEAD, THF, 60 °C, 10 h.

On the basis of the above-mentioned rationale, six diethers (±)-**1a**−(±)-**1f** containing acetamide functionalities at C7−OH and C20−OH of DHS were synthesized and the structural diversity of the amide moiety was incorporated into the designed analogues. Six alkenylated DHS derivatives (±)-**4a**−(±)-**4f** possessing various types of alkenyl substituents were also designed and prepared. The length of the alkenyl, the spatial distance between the double bond and the aromatic benzene A-ring, as well as the degree of alkenyl substitution, were all taken into consideration. Compound (±)-**2**, a monoether bearing only one acetamide moiety at C7−OH was prepared for comparison, especially with the corresponding diether (±)-**1a**. For more comparative information of those owning nonacetamide groups, compound (±)-**3**, a diacetylacetic acid ethyl esteric derivative of DHS was synthesized. To compare the influence of C23 hydroxyl substitutions, (±)-**5a** and (±)-**5b** esterified at C23 hydroxy group were prepared. The former (±)-**5a** possesses an electron-donating group at the substituent benzene ring, while the latter (±)-**5b** owns an electron-withdrawing 3-Cl-benzene moiety. All of the 16 synthesized DHS derivatives (Scheme 2), along with silybin and DHS, were subjected to 2,2-diphenyl-1-picrylhydrazyl (DPPH) and O_2^- free radical scavenging assays and an inhibition test against LPO. Subsequently, neuroprotective evaluation of the compounds against H_2O_2-induced toxicity of PC12 cells were performed in order to obtain more comprehensive knowledge of the DHS derivatives' in vitro efficacy against neuronal injury caused by oxidative damage.

Iron overload has long been associated with enhanced LPO,[54] and increasing reports associate chelation of ferrous ions (Fe^{2+}) with efficient therapy of AD.[55,56] The presence of metals may promote amyloid-β (Aβ) aggregates, whereas metal chelators can dissolve the proteinaceous tanglement from postmortem AD brain tissue and cerebral Aβ in the APP transgenic mouse model.[57] Specific metal-complexing agents may be a promising therapeutic strategy for AD.[58,59] In addition, numerous literature reports reveal cerebral microvascular injury resulting from xanthine oxidase (XO) production of superoxide free radicals.[60] XO inhibition is thereby implicated as another useful approach in treating cerebrovascular pathological changes or CNS diseases.[61,62] As such, we incorporated these two pharmacological models into the biological evaluation of the synthesized DHS analogues in order to identify potential correlations regarding antioxidant activities among different yet reliable screening models associated with AD and PD therapy.

Chemistry

Preparation of (±)-Silybin and (±)-Isosilybin. Large scale preparation of silybin was carried out to afford sufficient starting materials for the following modification and biological activity investigation. There are several reports regarding the synthesis and structural modification of silybin-like flavonolignans where DHS pentamethyl ether and dehydroisosilybin pentamethyl ether were prepared, followed by confirmation of the structure of silybin by comparing the NMR spectra of the compounds.[63,64] Additionally, silybin could be prepared by using biomimetic synthesis, where the synthesized product was a mixture of regioisomer attributable to silybin and isosilybin with a ratio of 57:43 by HPLC.[65] The overall synthesis strategy of silybin started from 4-hydroxy-3-methoxymethoxy-benzaldehyde, which afforded a stereoisomeric mixture,[65] while isosilybin was obtained from 3-hydroxy-4-methoxymethoxy-benzaldehyde by the same synthetic approach.[66] Asymmetric synthesis of silybin was also carried out,[67] upon which the obtained chalcone was steroselectively epoxidized under the catalysis of BQdC, while the successive deprotection in HCl−MeOH solution afforded stereospecific (+)-2*R*,3*R* taxifolin. This enantiomeric-pure dihydroflavonol was coupled with coniferyl alcohol in anhydrous benzene−acetone solution under the catalysis of silver carbonate to afford 2*R*,3*R*(+)-silybin and 2*R*,3*R*(+)-isosilybin.[67]

In the present study, (±) silybin was synthesized as shown in Scheme 1. The ferulic acid ethyl ester **8** was prepared by condensation of 3-methoxy-4-hydroxybenzaldehyde with (carbethoxymethylene)-triphenylphosphorane.[68] Reduction of **8** with a complex composed of lithium aluminum hydride and aluminum trichloride at room temperature yielded coniferol **9**. Another intermediate, dihydroquercetin (±)-**13**, viz. (±)-taxifolin, was synthesized via four steps with a total yield of 40%. Protocatechualdehyde was protected by MOMCl to give **10**, which was then subjected to condensation with **14**, obtained by MOMCl protection of phloroacetophenone. The reaction afforded the chalcone **11** in a 77% yield. Further oxidation of the chalcone with alkaline hydrogen peroxide led to a smooth formation of the epoxide (±)-**12**. The reaction could be easily monitored by the variation of UV absorption of the two compounds. The epoxide (±)-**12** was susceptible to cyclization with the presence of HCl−MeOH to procure the target molecule, (±)-taxifolin **13**. Finally, the silver-catalyzed oxidative coupling of **9** and (±)-**13** was performed in the dry benzene−acetone solvent system, which afforded (±)-silybin and (±)-isosilybin in proportions of 69/31, which could be finally separated by repeated column chromatography over diverse chromatographic packing materials. The large coupling constants between H10 and H11 (J = 8.0 Hz) revealed the *trans*-configuration of the products at C10/C11 positions. All of the spectral and physical data of the final products (±)-silybin and (±)-isosilybin were in accordance with literature reports.[69]

Stereochemically, the obtained epoxide (±)-**12** may be mixture of enantiomers due to the epoxidation by active oxygen probably adopting either α or β attack of the chalcone.[70] Only *trans*-fused product of cyclization, viz (±)-taxifolin **13**, was obtained however, which could be easily identified by its large coupling constant between H2 and H3 (J = 11.6 Hz). This may be attributed to the relatively vigorous reaction conditions, such as high temperature and reaction time, as well as the acidic environment, which not only favors the performance of a SN_1 reaction but also allows the epimerization/racemization of 2,3-*cis* conformers becoming 2,3-*trans*.[70] The yielded 2,3-dihydroquercetin (±)-**13** might be either (+)-2*R*,3*R*-*trans* or (−)-2*S*,3*S*-*trans* enantiomers.[70] Moreover, the obtained oxidative-coupling products with coniferol may also possess both 10*R*,11*R* and 10*S*,11*S* conformers, viz silybin A and silybin B.[28,69]

Synthesis of Dehydro-Silybin Derivatives. Scheme 2 illustrates the preparation of compound sets (±)-**1** to (±)-**5**. Among the five OH groups of silybin, C7−OH and C20−OH were more acidic than its counterparts. Thus, these two phenolic hydroxyls were more liable to alkylation in the presence of base. When silybin was subjected to reaction with various substituted 2-bromoacetamides **7** in the presence of K_2CO_3, C7,20-diethers were mainly obtained along with small amounts of 7-monoether as a byproduct. Therefore, (±)-**2** was neatly achieved with a reduced equivalent amount of **7a** (Scheme 2). Because the reaction conditions of path a and path b shown in Scheme 2 are quite similar, the equivalent amount of the bromoacetamides played a key role in differentiating the formation of either a monoether or a C7,20-diether. Furthermore, the monoetherification selectively occurred on C7−OH, which may be attributable to the fact that the proton of C7−OH is more acidic and less sterically hindered when compared with C20−OH. The predominant target products of amidation were found to be 2,3-dehydrogenated silybin derivatives. This indicated that silybin easily underwent oxidative dehydrogenation under this reaction condition due to the sensitivity of the flavonol nucleus toward base. This was further evidenced by the fact that silybin could also be transformed smoothly to DHS under this reaction condition without the presence of bromide **7**. Hence, the obtained compounds (±)-**1a**−**f** and (±)-**2** were 2,3-dehydrosilybin-7,20-diethers and 2,3-dehydrosilybin-7-monoether, respectively, which were confirmed by their NMR and mass data. Compound (±)-**3** was also obtained as a DHS derivative in a similar basic environment via reaction of silybin with excessive amount of ethyl chloroacetate.

Introduction of alkenyl groups to the skeleton of silybin showed some similarities to the above-mentioned modification reactions. The electrophilic substitution reaction concentrated on phenolic hydroxyls at C7 and C20 as expected. However, catalysis from KI could be omitted in the alkenylation reaction. Moreover, the equivalent amount of alkenyl bromide may also influence the reaction position on DHS. The monoether such as (±)-**4f** was obtained as the major product when the proportion of alkenyl bromide to silybin was <1. Reaction of silybin with ca. 2.2 equiv of alkenyl bromide smoothly provided the expected diether, although a small amount of monoether could also be traced. Prolonging the reaction time would reduce the monoalkenylated product, but the yield of the target diether was simultaneously decreased. Similarly, although raising the reaction temperature may quickly provide an optimum yield of the target diether, the complexity of the products increased. Interestingly, the general yields of the alkenylated products were lower than that of silybin reacted with bromoacetamides. This might be due to the better stability of the acetamides compared to the yielded alkenyl analogues, which ensures relatively high acetamide recovery during the reaction and workup process. Several successful experiments suggested that a rapid workup in a dark environment under nitrogen

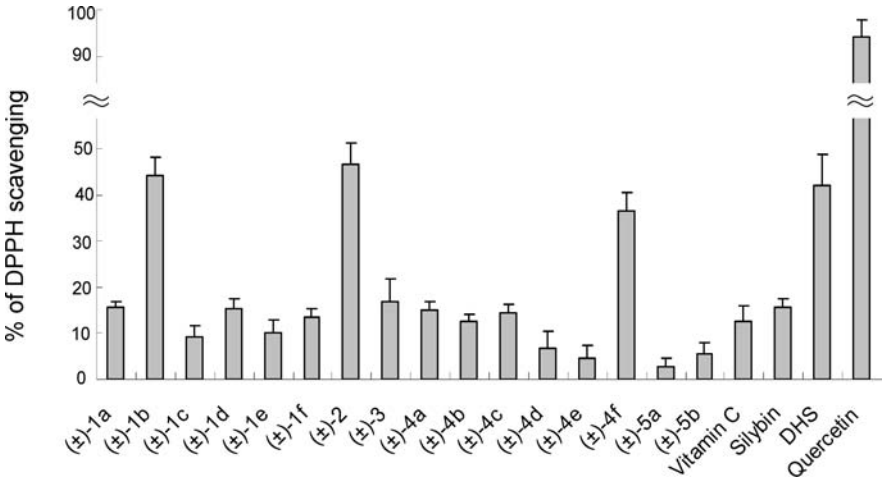

Figure 1. DPPH free radical scavenging activities of designed DHS derivatives (±)-**1**−(±)-**5** and reference compounds at 50 μM concentration. Data are expressed as the mean ± SD, $n = 3$ (EC_{50} of quercetin on DPPH radical scavenging was 3.4 ± 1.4 μM).

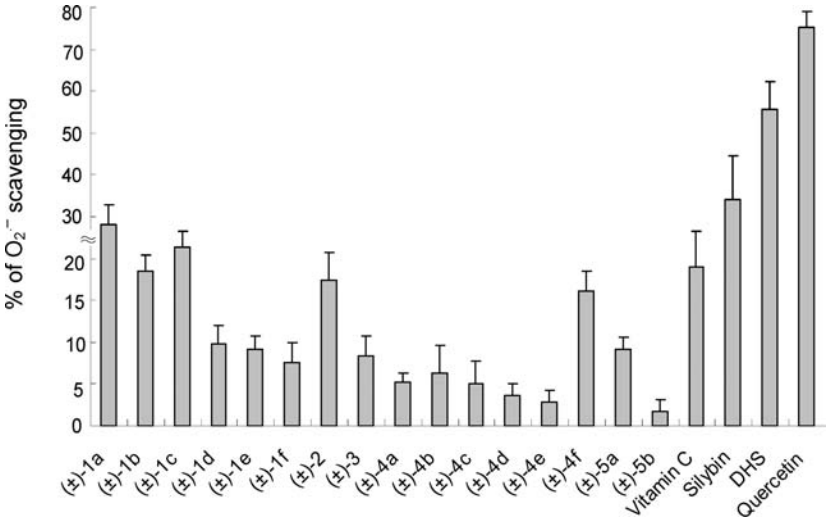

Figure 2. Superoxide anion free radical scavenging activities of designed DHS derivatives (±)-**1**−(±)-**5** and reference compounds at 50 μM concentration. Data are expressed as the mean ± SD, $n = 3$ (EC_{50} of quercetin on O_2^- radical scavenging was 38.6 ± 4.2 μM).

may increase the yield of the target alkenylated DHS analogues.

Compounds (±)-**5a** and (±)-**5b** were prepared by direct condensation of silybin with substituted benzoic acids in the presence of TPP and DEAD. Under elevated temperature at 60 °C, the two monoesters, (±)-**5a** and (±)-**5b**, were furnished and their structures elucidated by ^{1}H NMR and mass data (see Experimental Section). The downfield shift of H23 suggested that the esterification occurred at the sole methylene hydroxyl of silybin. Furthermore, (±)-**5a** and (±)-**5b** lacked another two downfield signals attributable to H2 and H3 in the case of silybin, which indicated that dehydrogenation also proceeded during the reaction. In our previous investigation of silybin derivatives, the C23 ester of silybin was achieved under much milder reaction conditions.[28] Therefore, it was evident that the elevated reaction temperature and prolonged reaction time ensured formation of the C23-esterified DHS analogues.

It should be mentioned that all of the target DHS ethers (±)-**1** to (±)-**5** were not subject to X-ray diffraction because of the difficulty in cultivating single crystals. However, by the typically large coupling constants between H10 and H11 exhibited around 8.0 Hz within these compound sets (see Experimental Section), it was unambiguous that we were dealing with the C10/C11-*trans*-configurated enantiomers of DHS. HPLC analysis also revealed that the products were single compounds with purity over 95%. Nevertheless, without the X-ray or CD spectra data, the absolute stereochemistry of the obtained DHS ethers remained undetermined.[69] The symbol of (±) was adopted for naming these DHS ethers to represent they should be either 10*R*,11*R* or 10*S*,11*S* stereoisomers. However, the determination of the absolute stereochemistry did not influence the preliminary SAR investigations in the present study, as CD and single crystal X-ray diffraction experiments of the DHS analogues should be performed for determination of their absolute stereochemistry when substantial pharmacological applications of these compounds are achieved.

Results and Discussion

Free Radical Scavenging Capacity of DHS Analogues. Bleaching of DPPH free radicals is a widely adopted assay to evaluate the scavenging potential of stable free radicals in vitro. From the results shown in Figure 1, we observed that introducing an amide group in (±)-**1** or an alkenyl chain in (±)-**4** at C20 of DHS led to a general reduction of quenching

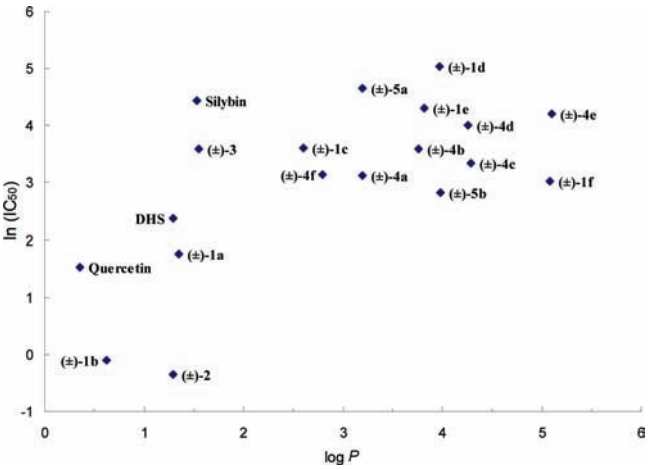

Figure 3. Correlation of Log *P* (partition coefficients) and ln (IC_{50}) for anti-LPO. For compound set (±)-**4**, DHS, and quercetin, 93% of the variance of ln (IC_{50}) could be explained by the factor of Log *P* alone.

ability against DPPH radicals when compared to DHS. Only the pyrrolidine derivative (±)-**1b** did not experience a C20 substituted reduction in activity compared to DHS and exhibited 44.2 ± 3.8% inhibition of DPPH radicals at the test concentration of 50 μM (Figure 1). Compound (±)-**1b** saw two times more DPPH scavenging compared to its *N*,*N*-diethyl substituted counterpart (±)-**1a** and would be consistent with the known DPPH scavenging properties of prolyl groups. The C20−OH functionality on the E-ring seems to play a key role in DPPH scavenging among DHS analogues, which was in agreement with previous investigations of methylated DHS derivatives.[33,36] Accordingly, the two analogues possessing accessible phenolic hydroxyls on the E-ring, (±)-**2** and (±)-**4f**, exhibited stronger scavenging effects compared with other analogues, and (±)-**2** (46.4 ± 4.4% inhibition) was found to be slightly more effective than DHS (42.2 ± 6.4% inhibition) ($p < 0.005$) (Figure 1). Compound (±)-**2** results support the argument that the phenolic C7−OH of DHS is not highly influential on DPPH scavenging properties of DHS,[33] which itself exhibited better scavenging ability compared to silybin in our study, consistent with previous reports.[22,36] Nevertheless, all the prepared DHS analogues demonstrated less quenching of DPPH radicals compared to the positive control quercetin. Vitamin C as a reference, exhibited weak activity (12.6 ± 3.4% at 50 μM) against DPPH radicals.

Superoxide anion radicals (O_2^-), a highly active type of ROS species, possess an unpaired electron prone to capture electrons from other molecules to form hydrogen peroxide that may further convert to hydroxyl radicals. All of the prepared DHS derivatives were subjected to O_2^- scavenging assay. It was discovered that amidation and alkenylation of DHS decreased the scavenging ability of the derivatives against O_2^- (Figure 2). This was not consistent, however, with the experimental results of di-*O*-allyl-magnolol, in which the introduction of the *O*-allyl group into magnolol unambiguously enhanced the O_2^- quenching capability compared to the parent magnolol, owning exposed free phenol groups.[50] Results for (±)-**2** and (±)-**4f** relative to other analogues again indicated that the phenolic hydroxyl in the aromatic E-ring of DHS may play a critical role in scavenging O_2^- radicals, as observed with the DPPH scavenging assay. The findings were also inconsistent with previous

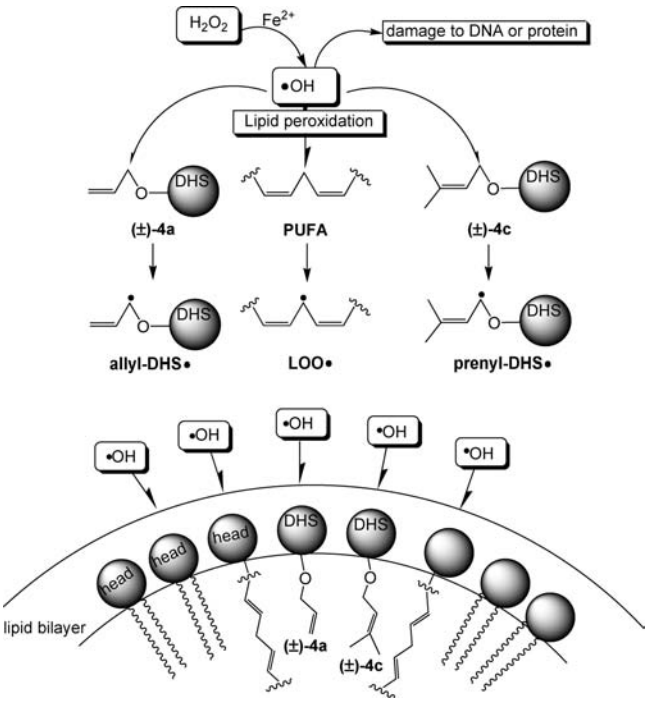

Figure 4. Hypothesized competition between PUFA and rational designed alkenylated DHS by a "flood-diversion outlet of free radicals" pattern in the LPO process.

work where introduction of an allyl or an (*E*)-2-propenyl group into a neolignan molecule strengthens the quenching ability toward O_2^- free radicals.[71] This might be attributable to the lipophilic substituents' covalent binding directly on the benzene skeleton, which may influence the electron density of the aromatic ring, thereby altering the free radical scavenging efficacy. The discrepancy of the results reported in different investigations might be due to the different models utilized. The O_2^- release in the latter study was from human polymorphonuclear leukocytes, which is believed to be associated with drug lipophilicity,[71] and higher lipid solubility favors the molecule entering the cell membrane where O_2^- is produced by membrane oxidases.[23,71−73] It is noteworthy that the scavenging capabilities of DHS analogues against DPPH and O_2^- radicals revealed unequivalent effects against two types of free radicals. This might be attributable to the different sizes of the radicals as well as the distinct inhibitory mechanisms with the molecules.[74]

Inhibition of LPO in Rat Liver Homogenates and SAR Discussion. Free radicals, such as hydroxyl and hydroperoxyl radicals can attack polyunsaturated fatty acids (PUFA) in the biomembrane and initiate LPO chain reactions, leading to membrane dysfunction and damage to local enzymes. Malonic dialdehyde (MDA) has long been used as a particular biomarker of oxidative stress, and an increase in MDA reflects LPO progression. In the present study, antiperoxidation effects of silybin derivatives on rat liver homogenates were evaluated by measuring lipid-derived MDA. The anti-LPO results of the prepared DHS analogues are shown in Table 1 and Figure 3 and revealed that both the strongest (±)-**1b** and weakest (±)-**1d** LPO inhibitors among the modified DHS derivatives were amidated analogues. The alkenylated analogues (±)-**4a**−**f** retained their ability to inhibit LPO compared to silybin (IC_{50} = 84.8 ± 5.3 μM), with IC_{50} values ranging from 22.6 to 67.5 μM, but were not stronger than DHS.

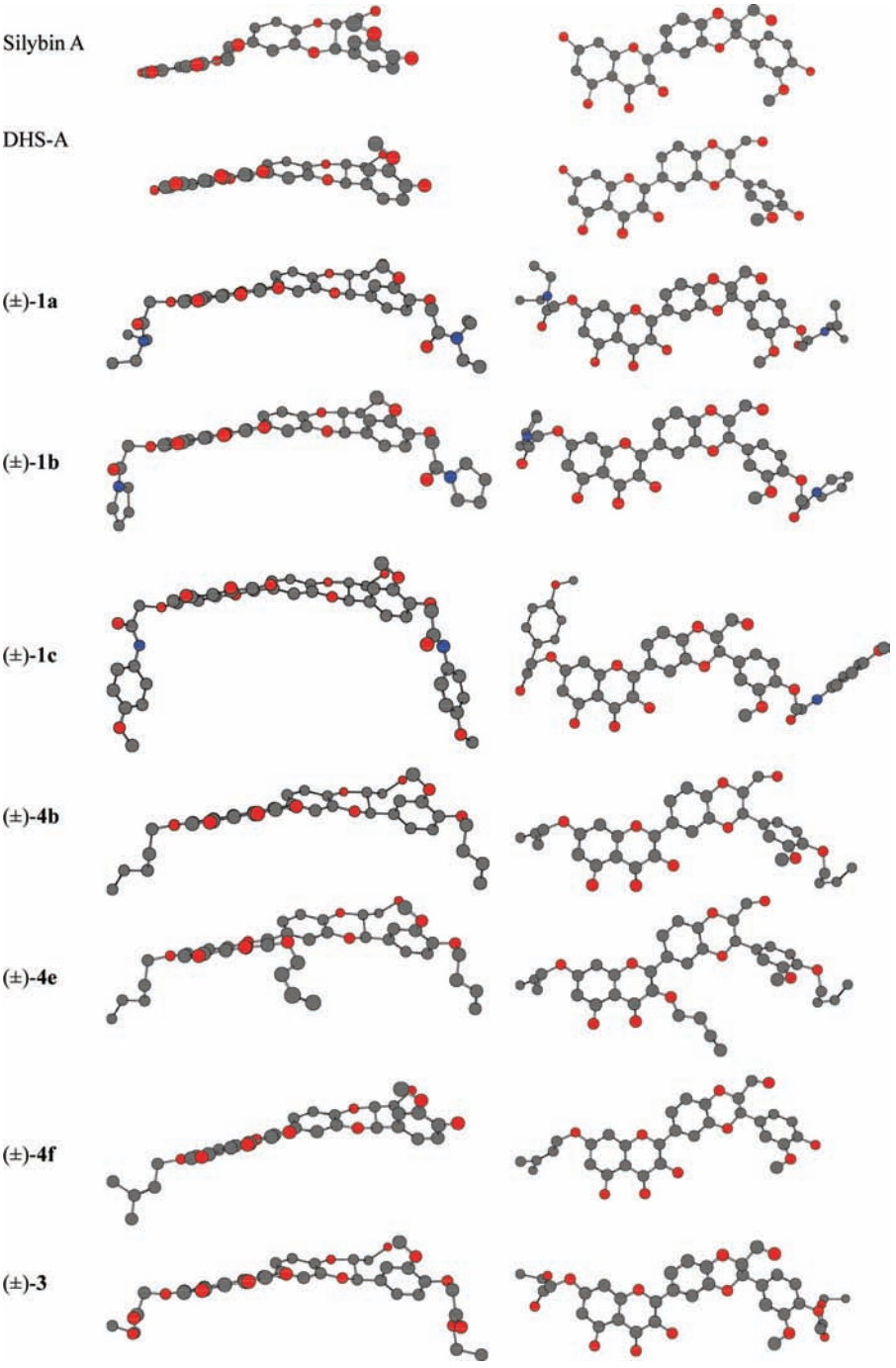

Figure 5. Energy-minimized 3D diagram comparisons of silybin A, DHS-A, (±)-**1a**, (±)-**1b**, (±)-**1c**, (±)-**3**, (±)-**4b**, (±)-**4e**, and (±)-**4f**. Left column shows the coplanar perspective of the A/B/C/D ring system of the compounds, and the right column shows the perpendicular view on the A/B/C/D plane of the compounds. DHS-A means dehydrosilybin A.

Figure 4 demonstrates the rational design hypothesis for the alkenylated DHS analogues exampled by (±)-**4a** and (±)-**4c**, as they may forge a competition with PUFA for acceptance of $^{\bullet}$OH radicals. Therefore, the presence of alkenylated DHS analogues could lead to consumption of $^{\bullet}$OH radicals, which originally prefer to attack the methylene position of the 1,4-pentadiene moiety of PUFA (Figure 4). This premise is supported by previous reports wherein prenylated compounds exhibited remarkable anti-LPO properties.[48] Among these experiments, H_2O_2 plays a role as an intermediate in the production of active ROS and may penetrate biological membranes and form harmful $^{\bullet}$OH radicals via catalysis of transition metals.[75] The attack to the liposomal bilayer may cause the deformation, rigidification, or linkage of lipid PUFA. However, the attack could be attenuated by the competitory radical acceptors of the alkenylated DHS analogues as illustrated in Figure 4.

In our study, increasing lipophilicity of alkenyl groups in (±)-**4** led to an apparent reduction in compound potency against LPO (Figure 3). The anti-LPO potency of set (±)-**4** was inversely correlated with Log *P* (r = 0.84). The correlation would be stronger except that di-*O*-prenylated (±)-**4c** (although more lipophilic) exhibited better anti-LPO potency than the observed set (±)-**4** trend, however was

not quite as potent ($p < 0.0005$) as its mono-*O*-prenylated counterpart (±)-**4f**. Alternately, the exposed C20−OH functionality in (±)-**4f** may be a factor in the slight (but statistically significant) improvement in potency over its C20 *O*-prenylated counterpart in (±)-**4c** (see compound (±)-**2** results) and raises the hypothesis that the SAR for LPO inhibition and DPPH radical scavenging may be related. Overall, the results may be analogous to an anti-LPO study on a 2,5-dihydroxy-4,6-dimethoxy-acetophenone structure where lipophilic C5-allyation of the phenolic hydroxyl causes a dramatic reduction in anti-LPO potency.[76] On the other hand, it was reported that alkylation at C3−OH causes enhanced potency,[77] whereas in our study, alkylation in compounds (±)-**4d** and (±)-**4e** showed a reduced effect. Inconsistent with our results is the report that replacing C7−OH of the flavone myricetin with alkyl chains of varying lengths (i.e., increasing lipophilicity) leads to improved potency against LPO.[78] It was therefore part of our rational design that an optimal degree of alkyl substitution would be favorable toward inhibition of LPO. In this study, trialkenylation of DHS analogues (±)-**4d** and (±)-**4e** enhanced their lipophilicity (which would increase their ability to access phospholipid sites), however bulky substituents enlarged the torsion angle between the planar A/C ring system and ring B, which may lead to loss of conjugation and an offsetting decrease in radical-trapping activity of the compounds. Additionally, the branched C3−OH alkenylated side chain "arms" may hinder the C7−OH substituent anchoring into the cell membrane and the hydroxyl groups may therefore not occupy the same spatial distribution at the membrane surface compared to DHS (Figures 4 and 5). This may partially explain the observation that the trialkenylated (±)-**4d** and (±)-**4e** only exhibit mild anti-LPO effects compared to other di- or monoalkenylated analogues.

The SAR for anti-LPO effects of the amidated DHS analogues could be obtained from analysis of the results displayed in Table 1 and Figure 3. Compound (±)-**1b**, an aliphatic substituted acetamide exhibited significant inhibition of LPO ($IC_{50} = 0.9 \pm 0.4\ \mu M$), 93 times lower than silybin ($IC_{50} = 84.8 \pm 5.3\ \mu M$), 11 times stronger than DHS ($IC_{50} = 10.7 \pm 1.7\ \mu M$), and most impressively, 5 times more active than quercetin ($IC_{50} = 4.6 \pm 1.8\ \mu M$). Another DHS derivative possessing the aliphatic *N*,*N*-diethyl-acetamidated moiety (±)-**1a** also demonstrated remarkable inhibition against LPO ($IC_{50} = 5.8 \pm 0.6\ \mu M$), stronger than that of DHS. However, those analogues possessing aromatic substituents on the amide nitrogen failed to exhibit inhibition comparable to the aliphatic amides (±)-**1a**, (±)-**1b** and (±)-**2**. The results suggested that introduction of aromatic functionalities to the amide moiety would remarkably reduce the inhibitory efficiency on LPO, while aliphatic acetamide substituents may increase the potency of the synthesized compounds against LPO. This result was similar to previous studies on lipoxygenase inhibition in which introduction of an aromatic ring to the amide group reduces the inhibitory effect on lipoxygenase when compared to those compounds receiving an aliphatic ring substituent on the amide.[51] The reason for improved aliphatic vs aromatic efficiency might be taken from the hypothesis that the aliphatic chain may undergo α-oxidation to form an oxidized product, which is subsequently prone to accept •OH radicals, constituting a delocalized steady state (Figure 6).[44] This explanation provided the rational background for our design of acetamidated derivatives, viz introducing the aliphatic amide into

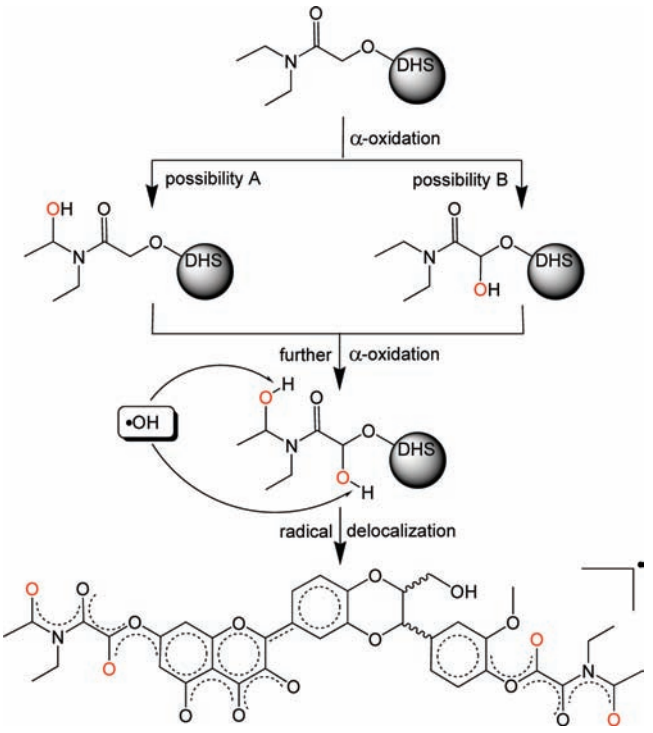

Figure 6. Possible delocalization (transition state) of amidated DHS analogue (±)-**1a** presented in the •OH free radical quenching process associated with LPO inhibition.

DHS might elevate anti-LPO activity. This logic was further supported by the observation that (±)-**2** containing a mono C7-*O*-*N*,*N*-diethyl-acetamide moiety displayed the best LPO inhibition ($IC_{50} = 0.7 \pm 0.2\ \mu M$) among the test compounds and reference substances (including quercetin). Comparison of the activity of (±)-**2** to DHS led to the reasoning that regiospecific introduction of an aliphatic acetamide moiety at C7−OH can significantly enhance the effects of DHS against LPO. Conversely, dual acetamide groups at C7 and C20 in (±)-**1a** led to a reduction in potency and supported a positive role for the exposed C20−OH functionality in (±)-**2**. Introducing aliphatic rigidity at C7/20−OH in (±)-**1b** however restored significantly enhanced activity to the molecule, although it is unknown if the SAR of the enhanced potency in (±)-**1b** is associated with the improvement seen in (±)-**2**. Compound (±)-**1a** was still almost 2 times more potent than DHS ($p < 0.0005$) and raised the hypothesis of a dominant role of C7 aliphatic acetamidation in LPO inhibition. Lastly, the dramatic reduction in activity for C7-*O*-monoprenylated (±)-**4f** when compared to the C7-*O*-monoacetamide (±)-**2** provided some initial empirical evidence that the aliphatic amide at C7 is a key functional group owing to enhanced anti-LPO effects of DHS.

It was observed that (±)-**1b** and (±)-**2** displayed concentration-dependent inhibition of LPO (Figure 7). The greater potency over DHS and quercetin yet their similar lipophilicity suggested that these aliphatic acetamidated DHS analogues may possess more affinity for the lipid peroxyl radicals than DHS and quercetin. Likewise, both (±)-**1b** and (±)-**2** exhibited stronger efficacy than DHS and quercetin at higher concentrations.

The diesteric ether (±)-**3** exhibited LPO inhibition ($IC_{50} = 36.4 \pm 4.6\ \mu M$) that remained more effective than silybin but was weaker than quercetin and DHS (Table 1). The two C23 esterified DHS analogues, (±)-**5a** and (±)-**5b**, exhibited

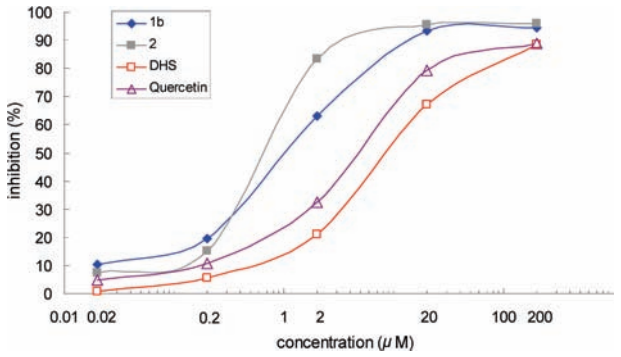

Figure 7. Concentration−response inhibitory effects against Fe^{2+}-mediated peroxidation of rat liver homogenates of (±)-**1b**, (±)-**2** and reference compounds DHS and quercetin. Data are expressed as mean of three independent experiments. ◆ = (±)-**1b**, ■ = (±)-**2**, □ = DHS, and △ = quercetin.

divergent activities against LPO with IC_{50} values of 104.2 ± 9.6 and 16.9 ± 2.0 μM, respectively. It is unknown whether an electron withdrawing substituent at the phenyl ring is responsible for the apparent increased potency of (±)-**5b** relative to (±)-**5a**, as the results were in contrast to recent studies by our group, which revealed no significant reduction in potency against LPO for silybin C23 electron-donating trimethoxylated esters and suggests a potentially different SAR for the 2,3-dehydrosilybin vs silybin.[28] Interestingly, DHS exhibited roughly 8 times more inhibition of LPO than silybin, which is to a certain extent in agreement with previously reported results.[22]

The overall relationship of Log *P* and ln(IC_{50}) of anti-LPO effects for the tested compounds is shown in Figure 3. The data shows an inverse parabolic relationship between compound potency and lipophilicity for all tested compounds, where unexpectedly the five most active anti-LPO compounds were also the least lipophilic. A prominent inverse linear correlation ($r = 0.98$) was found in compound series (±)-**1** excluding (±)-**1f**. It is reasonable that dual electron-withdrawing substitutions in (±)-**1f** (although more lipophilic) may reduce the electron density of the aromatic rings, which based on the above SAR results would have contributed to some restored activity in (±)-**1f**. The correlation coefficient for (±)-**1** including (±)-**1f** was 0.78. Although both (±)-**1** and (±)-**4** showed inverse correlations of lipophilicity with activity, the influence of lipophilicity on potency was 3 times more sensitive for (±)-**1** than (±)-**4** (slope parameter = 0.59, $p < 0.005$ vs 0.19, $p < 0.05$). This indicated that aromatic-based increases in lipophilicity may cause greater reductions in potency than would alkenyl-based increases in lipophilicity for DHS analogues. Other investigators have also reported negative correlations or diminished abilities to inhibit LPO with increasing lipophilicity.[79,80] The inverse relationship observed indicates that anti-LPO activity of the analogues in this study was not primarily dependent on access to phospholipid sites of peroxidation. In all, the results suggested that inhibition of LPO was not only associated with trapping $^{\bullet}OH$ radicals but also enzymology cofactors or undefined action systems. This deduction is supported by the observation that a C7 side chain flavone possesses better inhibition against LPO than those analogues possessing C8 side chains,[70,76] which raises the hypothesis that conformation and orientation of active substituents are potentially more influential than lipophilicity in LPO inhibition.

Table 1. Inhibitory Effects of Compounds Sets (±)-**1**−(±)-**5** and Positive Controls on Rat Liver Homogenates Lipid Peroxidation [a]

compd	lipid peroxidation inhibition, IC_{50} (μM)
(±)-**1a**	5.8 ± 0.6
(±)-**1b**	0.9 ± 0.4
(±)-**1c**	37.0 ± 2.7
(±)-**1d**	152.7 ± 10.8
(±)-**1e**	74.1 ± 6.9
(±)-**1f**	20.7 ± 2.7
(±)-**2**	0.7 ± 0.2
(±)-**3**	36.4 ± 4.6
(±)-**4a**	22.6 ± 2.9
(±)-**4b**	36.2 ± 3.7
(±)-**4c**	28.1 ± 4.7
(±)-**4d**	54.8 ± 5.5
(±)-**4e**	67.5 ± 9.8
(±)-**4f**	23.3 ± 3.6
(±)-**5a**	104.2 ± 9.6
(±)-**5b**	16.9 ± 2.0
silybin	84.8 ± 5.3
DHS	10.7 ± 1.7
quercetin	4.6 ± 1.8

[a] Data are expressed as the mean ± SD, $n = 3$.

Ferrous Ion Chelation Properties of DHS Analogues. The anti-LPO effects of the amidated DHS analogues could be preliminarily relegated to a combination of structural features. First, trapping of harmful $^{\bullet}OH$ radicals by a conjugated delocalizing system may be an efficient way to deal with LPO. Additionally, taking into account the report that the dinitro-linker (N−C−C−N) in trolox−lipoic acid diamide hybrids plays a key role in suppression of iron-mediated LPO,[81] it was reasoned that amide oxygen chelation of Fe^{2+} might be a characteristic of amidated DHS analogues. To examine this potential effect in LPO inhibition, the prepared DHS analogues were subjected to Fe^{2+} chelation measurements. It is well accepted that H_2O_2 may penetrate cell membranes but not directly evoke LPO.[82] H_2O_2 can generate $^{\bullet}OH$ radicals when mediated by Fe^{2+}, subsequently inducing LPO.[83] Furthermore, the levels of Fe^{2+} in the brain of AD and PD patients have been found to be abnormally higher than healthy subjects. It is hypothesized that the Fe^{2+}-induced Fenton reaction elevates the probability of LPO on neuronal cells, together with the aggregation of Aβ.[83] Therefore, Fe^{2+} chelation may constitute one of the essential mechanisms of neuronal protection.[58,59,81] Our experiment adopted a nonenzymatic Vc−Fe^{2+} (ferrous sulfate/ascorbate) system to ensure that Fe^{3+} was reduced to Fe^{2+}. The Fe^{2+} chelating activities of the test compounds were assessed using the differences of absorbance at 562 nm, demonstrating inhibition of the ferrozine−Fe^{2+} complex. The percent inhibition of the ferrozine−Fe^{2+} reaction is indicative of the stability of Fe^{2+} complexes by the test compounds.

The compounds unveiled Fe^{2+} chelation activities that showed a linear correlation ($r = 0.66$, $p < 0.005$) with the results against LPO (Table 1 and Figure 8), providing evidence that Fe^{2+} chelation activity is associated with the observed anti-LPO potency of the DHS analogues. Compound (±)-**1b** again demonstrated the most potent activity in Fe^{2+} chelation (EC_{50} = 23.2 ± 1.8 μM, 87% inhibition) and was over 2 times more potent than (±)-**1a** (EC_{50} = 59.9 ± 6.2 μM, 63% inhibition) as seen with the LPO inhibition and DPPH scavenging results. Compound (±)-**1b** was 4 times more potent in Fe^{2+} chelation compared to DHS

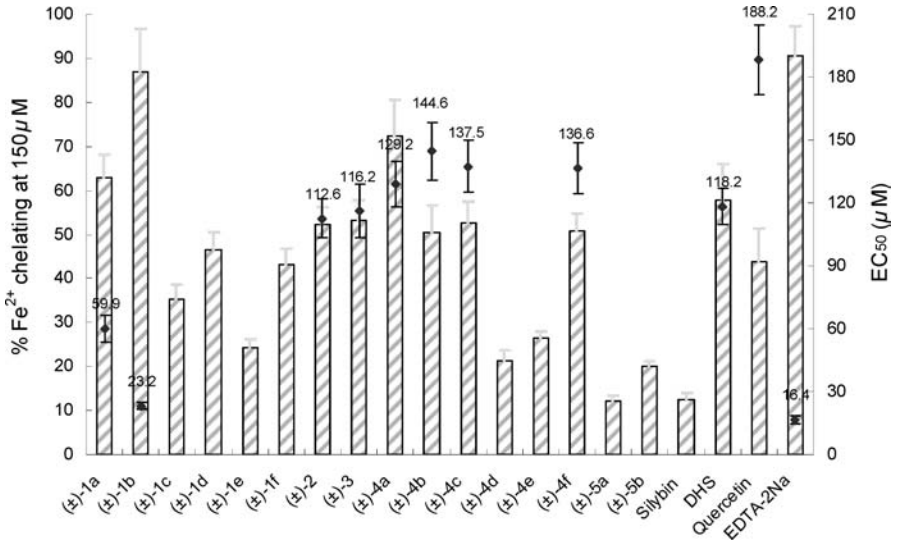

Figure 8. Fe^{2+} chelating activities of (±)-**1**−(±)-**5** and reference compounds silybin, DHS, quercetin, and EDTA-2Na. The height of each bar represents the percentage of Fe^{2+} chelated by corresponding compounds at the concentration of 150 μM. The symbol "◆" denotes that EC_{50} was generated for those compounds that reached 50% Fe^{2+} chelation and are shown on the secondary *y*-axis. Data are expressed as the mean ± SD, $n = 3$.

(EC_{50} = 118.2 ± 8.6 μM, 58% inhibition) and 7 times stronger than quercetin (EC_{50} = 188.2 ± 16.7 μM, 43.5% inhibition). Compound (±)-**2** was the next strongest analogue at Fe^{2+} chelation (EC_{50} = 112.6 ± 9.5 μM, 52.5% inhibition), which was similar to the Fe^{2+} chelation properties of DHS. Compounds (±)-**1a**, (±)-**1b**, (±)-**2**, and DHS thus demonstrated a different heirachy in Fe^{2+} chelation ((±)-**1b** > (±)-**1a** > (±)-**2** ≈ DHS) than that seen in LPO inhibition ((±)-**1b** ≈ (±)-**2** > (±)-**1a** > DHS) and DPPH free radical scavenging ((±)-**2** > DHS ≈ (±)-**1a** > (±)-**1b**).

It was previously determined that the iron chelaton binding site in quercetin[84] and silybin[85] utilize the carbonyl oxygen and α-secondary hydroxyl group on C3 and C4 as bidentate donor groups, and thus the dramatically stronger chelation ability of DHS over silybin is associated with C2,3-desaturation. Assuming silybin−iron complexation is limited to the C ring (i.e., the lignin portion of the molecule is not believed to participate in chelating iron),[85] then the improved chelation properties of DHS over quercetin is not easily explained and implicates a potential larger dilution effect for quercetin at lower concentrations and/or favorable geometric arrangement for DHS molecules (i.e., the coordination number for Fe^{2+} is 4 oxygens). For DHS analogues, the improved potency of (±)-**1a** compared to DHS suggests that the aliphatic substituted acetamides may be multidentate ligands compared to the monodentate ligands DHS and silybin. The rigid pyrrolidine substitutions in (±)-**1b** also apparently created more stable iron complexes (i.e., % ferrozine−Fe^{2+} complex inhibition) compared to the more flexible *N*,*N*-diethyl-acetamidated (±)-**1a**. Because the spectrophotometric assay is stoichiometric, the higher potency of (±)-**1b** denotes less compound bound per metal equivalent (i.e., a lower ligand−metal ratio) and (±)-**1b** may have been less dependent on the 3D molecular arrangement for stability and/or less susceptible to a dilution effect. The higher potency would also be explainable if (±)-**1b** was more sensitive than (±)-**1a** to α-oxidation by soluble O_2 or trace Fe^{3+} was able to be generated in the presence of ascorbate. By comparison, EDTA-2Na provided three deprotonated acetate groups in this assay (out of four total) and was expected to donate the most carboxyl oxygens available for chelating Fe^{2+}. Compound (±)-**2** possesses only one aliphatic amide, which could account for the weaker EC_{50} compared to (±)-**1a** and (±)-**1b** but does not readily account for the similar results to DHS (Figure 8). In all, it appears the Fenton reaction may be effectively blocked by these proposed multidentate ligand DHS analogues and may have contributed to the observed efficacy against LPO. The potency of (±)-**2** in Fe^{2+} chelation, however, was not comparable to (±)-**1b** as seen with LPO inhibition and reinforced the proposal that LPO inhibition is not solely dependent on Fe^{2+} chelation but rather consists of varied or multiple action systems.

The acetamide derivatives (±)-**1c**−(±)-**1e** possessing aromatic rings failed to show substantial chelating efficacy on Fe^{2+} when compared with (±)-**1a** and (±)-**1b** (Figure 8). One postulate is that the aromatic ring may reduce the nucleophilicity of the amide carbonyl group by resonance. The diesteric ether (±)-**3** also displayed moderate activity toward Fe^{2+} chelation (EC_{50} = 116.2 ± 12.7 μM, 53.5% inhibition) but not significantly better than that of DHS. Compared to (±)-**1a**, the potential chelator moiety at the carboxyl oxygen atoms of C7/20 in (±)-**3** is perhaps less stable for iron complexation than amide chelators, as seen with hydroxamate groups in siderophore chemistry. As expected, the C23 esters (±)-**5a** and (±)-**5b** containing no affordable C7/20 chelation donors in the molecules exhibited rather weak chelating capacity. The C2,3-desaturated (±)-**5a** however was even less reactive than silybin and provides a hypothesis that favorable molecular packing is essential in the chelation effects of DHS analogues or lignoflavonoids. Considering (±)-**5b** exhibited 5 times stronger anti-LPO activity than (±)-**5a** (Table 1), this further supports a theory of complexity in LPO inhibition.

The general chelating potency of the alkenylated DHS analogues of set (±)-**4** was weaker than the acetamide analogues (±)-**1a** and (±)-**1b** (Figure 8). Compounds (±)-**4b**,**c** and (±)-**4f**, however, displayed an apparent slight divergence between potency and efficacy compared to most other compounds. For instance, the C7-mono prenylated

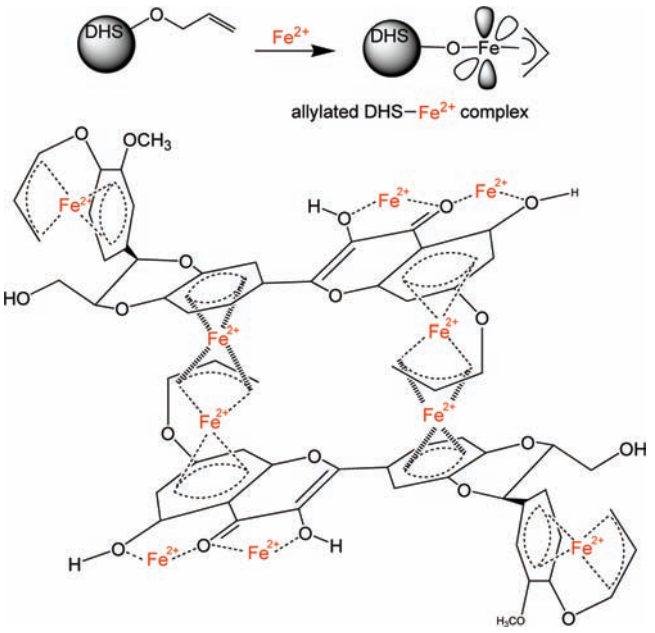

Figure 9. Imaginary $\pi-Fe^{2+}-\pi$ complex between the allyl π electrons and the π electrons of the aromatic rings due to DHS analogue (±)-**4a**, both of which acted on Fe^{2+}. The intramolecular complexation was illustrated by "---", while the intermolecular complexation was represented by "|||", respectively. The chelation of Fe^{2+} due to the 3-OH-4-oxo-5-OH core is also expressed in the diagram for comparison. Each (±)-**4a** molecule may consume 5 equiv of Fe^{2+} by the hypothesis described.

(±)-**4f** (EC_{50} = 136.6 ± 12.4 μM, 51% inhibition) displayed lower potency but relatively equivalent chelating efficacy at 150 μM compared to the C7-mono acetamidated (±)-**2** and suggested a potential dilution effect was strongest among the alkenylated compounds. It must also be considered that the geometric arrangement of monosubstituted analogues would not structurally allow more efficient Fe^{2+} chelation than DHS, although the conclusion would not be allowed based on two compounds (±)-**2** and(±)-**4f**. Compounds (±)-**4a**,**c** and (±)-**4f**, although generally less potent Fe^{2+} chelators compared to DHS, were more active than quercetin. The best Fe^{2+} chelator among the alkenylated group was the diallylated DHS (±)-**4a** (EC_{50} = 129.2 ± 10.8 μM), less potent than (±)-**1a**, (±)-**1b**, and DHS, but surprisingly more effective (72.5% inhibition) than both (±)-**1a** and DHS. This phenomenon represented a strong divergence in the correlation between Fe^{2+} chelation potency and inhibition efficacy (r = 0.99 drops to 0.91 including (±)-**4a**) among test compounds above 50% inhibition. The higher efficacy and lower potency relative to other compounds and typified by (±)-**4a** may be related to Fe^{2+} forming a complex with allyl ligand by stable bonding.[86] Consequently, a rational hypothesis describing Fe^{2+} chelation by (±)-**4a** was illustrated in Figure 9. It could be proposed that diallylated DHS (±)-**4a** may form an intramolecular $\pi-Fe^{2+}-\pi$ complex wherein the Fe^{2+} is within a clathrate-like environment and thereby stabilized between the allyl π electrons and the π electrons of the aromatic rings due to DHS (see Figure 9). An intermolecular $\pi-Fe^{2+}-\pi$ complex between two molecules may also be formed to diminish Fe^{2+} from the reaction system and thereby attenuate LPO. This reasoning may explain the relatively significant anti-LPO efficacy of (±)-**4a**. The trialkenylated DHS analogues (±)-**4d** and (±)-**4e** may not form the effective inter- or intramolecular $\pi-Fe^{2+}-\pi$ complex because of the overcrowded compactness of the alkenyl substituents, which affect the stretching of the molecules and thereby may have hindered chelation of Fe^{2+} (Figure 5). Compounds (±)-**4d** and (±)-**4e** (substituted at C3−OH) exhibited rather weak chelation of Fe^{2+} (Figure 8) and were no longer considered as potential lead compounds.

In summary, only a few DHS derivatives did not retain their chelating efficiency of Fe^{2+} ions compared to DHS, however, all remained superior to the known Fe^{2+} chelator silybin, which was able to inhibit ferrozine−Fe^{2+} complexation by 12.5% in our assay. Impressively, the best chelator among the test compounds (±)-**1b** was almost as effective in the ferrozine−Fe^{2+} inhibition assay as an aminopolycarboxylic acid (EDTA-2Na, EC_{50} = 16.4 ± 2.0 μM, 91.5% inhibition).

Neuron Protective Properties of DHS Analogues. Rat pheochromocytoma (PC12) cells have become increasingly popular as a screening model for assessing the prevention of ROS-induced neuronal death.[87] Cultured PC12 cells are commonly utilized to investigate neuronal protection for AD, PD, and progressive autosomal dominant neurodegenerative disorders such as Huntington's disease.[88−90] Cells exposed to H_2O_2 solution lead to abrupt shrinkage as well as apoptosis, while the protective effect on neuronal cells against oxidative stress may be conveniently evaluated for positive changes in cell viability using the MTT assay. The cell viabilities attributable to the protective efficiency of the test compounds in PC12 cells are listed in Figure 10. The aliphatic acetamide ethers (±)-**1a** and (±)-**1b** exhibited better effects in PC12 cell protection against H_2O_2-induced cell injury than the aromatic acetamide ethers (±)-**1c**−**f**, which was in agreement with the heirachy of set (±)-**1** LPO inhibition activity. In addition to the proposed mechanism in Figure 6, it is feasible that the DHS acetamides possessing an aromatic ring (±)-**1c**−**f** may reduce the possibility of forming hydrogen bond donors or acceptors compared with (±)-**1a** and (±)-**1b** owning activated nitrogen atoms near flexible and rigid aliphatic chains (Figure 5). PC12 cell protection was more effective at 50 μM for (±)-**2** and (±)-**4f** compared to (±)-**1a** and (±)-**4c**, respectively, suggestive that exposure of C20−OH in the E-ring continued to be favorable against ROS attack. Similar to the LPO inhibition assay, compound set (±)-**4** showed a very prominent inverse linear relationship (r = 0.99, p < 0.005) between neuronal protection and lipophilicity. Despite decreasing potency with lipophilicity in set (±)-**4**, the more lipophilic alkenylated compounds (±)-**4a**−**c** and (±)-**4f** surprisingly exhibited better PC12 cell protection compared to the more polar acetamidated compounds (±)-**1a** and (±)-**1b**. Moreover, compound (±)-**4a** (EC_{50} = 20.5 ± 3.4 μM) displayed greater potency in neuronal protection than DHS (EC_{50} = 30.2 ± 4.3 μM) and was consistent with Fe^{2+} chelation results in this study.

The positive neuroprotective effects of alkenylated over acetamidated DHS derivatives suggested an optimum degree of lipophilicity may be a dominant factor in whole cell antioxidant assays, however, no linear relationship was found between lipophilicity and cell protection for the tested compounds. Furthermore, increased lipophilicity would not account for the positive neuronal protective effects of DHS. We proposed that the size of the molecules relative to their polar surface area may have limited the cellular distribution of compounds (±)-**1a** and (±)-**1b**. It was found that the percent increase in PC12 cell viability at 50 μM for the

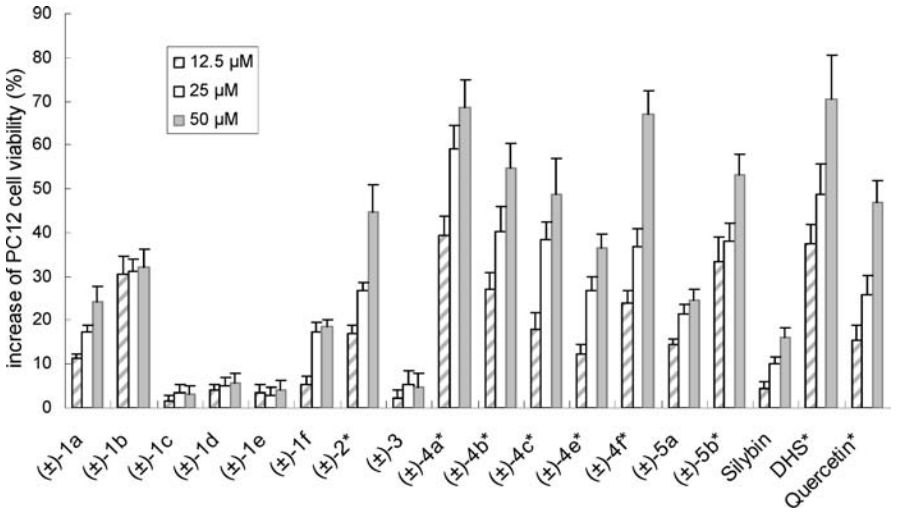

Figure 10. Increased cell viabilities by compounds (±)-**1a**−**f**, (±)-**2**−(±)-**4c**, (±)-**4e**−**f**, (±)-**5**, and reference compounds silybin, DHS, and quercetin measured at 12.5, 25, and 50 μM, respectively. Data are expressed as the mean ± SD, $n = 3$. The symbol "*" denotes that EC_{50} was generated for those compounds that reached a 40% increase in cell viability. EC_{50} values were (±)-**2** = 64.3 ± 7.1 μM, (±)-**4a** = 20.5 ± 3.4 μM, (±)-**4b** = 37.7 ± 3.1 μM, (±)-**4c** = 47.4 ± 3.7 μM, (±)-**4e** = 79.4 ± 8.3 μM, (±)-**4f** = 32.0 ± 4.4 μM, (±)-**5b** = 46.5 ± 5.2 μM, DHS = 30.2 ± 4.3 μM, quercetin = 58.4 ± 9.6 μM.

effective DHS derivatives showed a linear inverse correlation with the van der Waals polar surface area ($r = 0.93$, $p < 0.001$) but not other physicochemical or topographical indices tested. Correlations between the van der Waals polar surface area and brain penetration have been reported in the literature[91] and endorse the premise that (±)-**1a** and (±)-**1b**, although potent LPO inhibitors, may be ineffective at accessing sites of ROS production and are candidates for cellular-delivery formulations.

The diesteric ether (±)-**3** failed to offer protection of PC12 cells, which was inconsistent with its Fe^{2+} chelation and LPO inhibition activity. The C23 ester (±)-**5b**, possessing electron-withdrawing functionality on the aromatic substituent (EC_{50} = 46.5 ± 5.2 μM), appeared to be more effective in neuronal protection than (±)-**5a**, which owns an electron-donating substituent in the aromatic moiety and was consistent with the LPO inhibition results. This neuroprotective activity was impressively slightly better than quercetin (EC_{50} = 58.4 ± 9.6 μM). DHS was also more effective at neuronal protection compared to silybin and quercetin. Compounds (±)-**4d** and (±)-**4e** were not considered potential leads due to weak performance in other assays, and (±)-**4d** was removed from this study.

The results recurrently supported the conclusion that C2,3-desaturation in the silybin skeleton may be important in the neuronal protective efficacy of flavonoid and flavonolignan structures[33,92−94] Furthermore, the hypothesis that increased lipophilicities of DHS and its analogues confer better affinity to lipid bilayers and enhance competition with native lipids of the neuronal cell membrane is supported by compound set (±)-**4** (Figures 3 and 4). This competition may subsequently diminish cell membrane damage from H_2O_2-induced ROS attack (Figure 4). Overall, the findings are in agreement with the concept that lipophilicity of drug molecules is advantageous for efficacy in antioxidant and chelation therapy, especially for AD and PD patients where molecular transport through the blood−brain barrier is essential.[52,53,67] Nevertheless, the results comprehensively suggest the mechanism of PC12 cell protection afforded by the compounds is rather intricate and complex. Apart from the studied compound properties such as free radical scavenging, LPO inhibition, and Fe^{2+} chelation, the neuroprotective capability of the molecules might be attributable to other factors related to GPCR-mediated ERK, caspase-3 suppression, and/or overexpressed neuroglobin, which protects neuronal cells from ROS.[95−97] Likewise, the possibility exists for direct biochemical effects, as flavonoid-type compounds have been implicated in a number of neuronal protein kinase and lipid kinase signaling cascades.[98,99] Thus, definitive conclusions should be avoided regarding the mechanism of neuroprotective effects, and the lead homologues possessing the DHS template in this study should therefore be subjected to further detailed pharmacological investigations.

Xanthine Oxidase Inhibition Assay. XO inhibition measurements are a helpful method for determining ROS quenching and therefore act as an indicator of CNS protection from oxidative damage.[100] The activity of the test compounds against XO are shown in Figure 11. Consistent with results from other antioxidant screening models, silybin did not markedly inhibit XO, whereas DHS was more effective (IC_{50} = 80.3 ± 5.6 μM). Although significant XO inhibition was not observed among the acetamide DHS analogues, compounds (±)-**1a**, (±)-**1b**, as well as (±)-**2** (which possess aliphatic side chains) still exhibited stronger inhibition of XO compared to the aromatic acetamides (±)-**1c**−**f** and suggests a potential SAR in XO inhibition by flavonolignans. The degree of acetamide substitution in these molecules did not influence the strength of inhibition, as (±)-**2** showed very similar activity compared to (±)-**1a** and (±)-**1b** (Figure 11). Alkenylated analogues (±)-**4** did not exhibit remarkable suppression of XO in this assay. Compound (±)-**4c**, the best inhibitor in this series, displayed XO inhibition of 18.9 ± 2.6% at the test concentration of 75 μM. Only the diesteric ether (±)-**3** exhibited over 50% inhibition of XO among the DHS analogues in this study, with an IC_{50} of 70.8 ± 4.8 μM, less potent than allopurinol (IC_{50} = 21.2 ± 1.8 μM) but stronger than silybin and DHS (IC_{50} = 80.3 ± 5.6 μM). This suggested that an esterified ether moiety linked to phenolic C7−OH and C20−OH of DHS may have a positive impact on XO inhibition and provide a template for

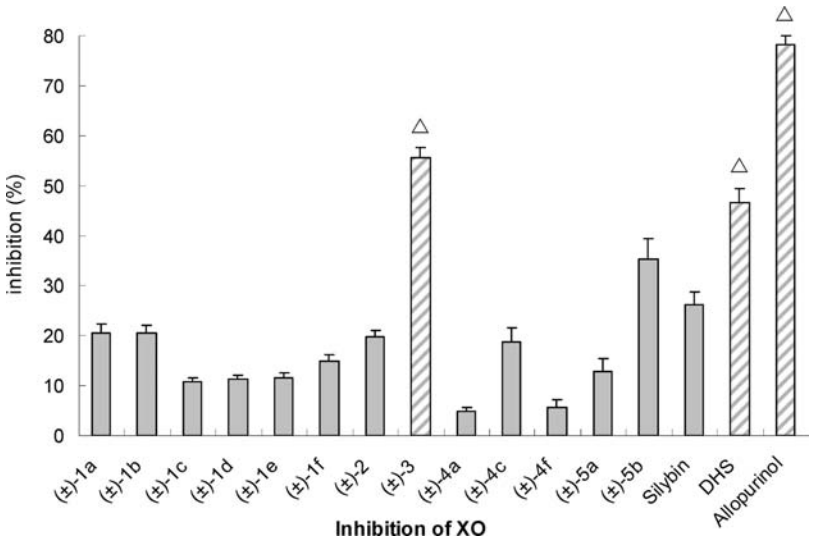

Figure 11. Inhibition of XO by by compounds (±)-**1a**−**f**, (±)-**2**, (±)-**3**, (±)-**4a**,**c**,**f**, (±)-**5**, and reference compounds silybin, DHS, and allopurinol at 75 μM concentration. The Data are expressed as the mean ± SD, $n = 3$. The symbol "△" denotes that IC_{50} was generated for those compounds that reached 50% of inhibition. The IC_{50} of (±)-**3**, DHS, and allopurinol were 70.8 ± 4.8, 80.3 ± 5.6, and 21.2 ± 1.8 μM, respectively.

ongoing SAR studies of DHS derivitaves. Previous SAR studies report that the planar C2,3-desaturation is essential for competitive binding to the active site of XO[101] and is consistent with the improved activity of DHS over silybin observed in our study. It was also reported that the C7−OH is essential for XO binding[102] and would account for the lack of potency observed in (±)-**4a** and other DHS analogues. However, both (±)-**3** and a C7 methyl-ether quercetin derivative[103] did not see significant reductions in potency compared to their parent structures, which was a deviation from other ineffective C7−OH substituted compounds. The C23 esterified DHS analogues (±)-**5a** and (±)-**5b** failed to perform compared to DHS, however (±)-**5b** again showed higher activity than its counterpart and remained more effective than silybin (Figure 11). The XO inhibition activity of (±)-**5b** shows an interesting correlation with previous antioxidant and neuroprotective assays in this study in that the C23 ester bearing an electron-withdrawing substituent was more active than the electron-donating-group-bearing analogue (±)-**5a**. Both DHS and the structurally modified analogues failed to match the XO inhibition activity of allopurinol. XO is a well-known producer of superoxide free radicals, and the overall XO inhibition properties in this assay matched the lack of O_2^- free radical scavenging ability of the DHS derivatives (Figure 2). However, considering that enzyme systems such as caspase-3, NADPH oxidase, lipoxygenase, and cycloxygenase may also be involved in ROS-related cell apoptosis, XO inhibition might be responsible for only a segment of the comprehensive antioxidant properties of the test compounds.[73,104]

Conclusion

In summary, this study disclosed that the diether at C7−OH and C20−OH as well as the monoether at C7−OH of DHS, which possess aliphatic substituted acetamide functionalities, demonstrated excellent inhibition against LPO as well remarkable chelating potency on Fe^{2+} ions. The diallyl ether at C7−OH and C20−OH of DHS exhibited significant protective ability of PC12 cells against H_2O_2-induced cell injury, which was more potent than the positive controls. The effects of aliphatic versus aromatic substituents and electron-donating versus electron-withdrawing groups on the tested pharmacological activities were also analyzed. In addition to DPPH, O_2^- scavenging, and LPO inhibition assays, we employed Fe^{2+} chelation and PC12 cells for the first time in the assessment of DHS and its analogues for their neuron protective effects from oxidative damage. The superior neuroprotective properties of DHS and some lipophilic DHS analogues when compared to silybin suggest that the van der Waals polar surface area of lignoflavonoids should be emphasized in future SAR studies, especially those using pathological screening models against CNS diseases such as AD and PD. Further systematic preparations of DHS and other silybin derivatives, along with multimodel screenings for cross-evidence of their pharmacological potential as antioxidant drugs with utility in CNS diseases, are currently in progress. The findings reported in the present study might serve as inputs into our understanding of prevention and treatment of the injuries, disorders, and diseases caused by reactive oxygen species and provide insights in future drug design and development for the treatment of neurodegenerative disorders such as AD and PD.

Experimental Section

General Experimental Procedures. PMS, NBT, hydrogen peroxide (H_2O_2), MTT, ferrozine, TBA, ferrozine, EDTA-2Na, quercetin, and xanthine were purchased from Sigma Chemical Co. (St. Louis, MO). Silybin as reference compound in the pharmacological experiments was purchased from Liaoning Panjin Pharmaceutical Co. Ltd. (Liaoning, China) as 98.5% purity by HPLC. HPLC analyses were performed on an Agilent 1100 system (Agilent Technologies, Palo Alto, CA) equipped with an autosampler. MeOH (HPLC-grade) was purchased from Ludu Chemical Reagent Factory (Shanghai, China). Trixon-100 and DMEM medium were obtained from Gibco (Grand Island, NY). Reduced NADH disodium salt was supplied from Amresco (Solon, OH). All other reagents were of the highest purity commercially available. The rat pheochromocytoma (PC12) cell line was obtained from the Shanghai Institute of Cell Biology, Chinese Academy of Sciences. Sprague−Dawley rats for harvesting livers were obtained from

the Zhejiang Center of Laboratory Animals, China. The use of animals was in accordance with Guidelines for the Care and Use of Laboratory Animals of Zhejiang University. OD values were analyzed on an ELISA plate reader from Bio-Tek Instruments (Winooski, VT). Statistical differences between synthesized compounds and DHS were analyzed by the paired *t* test.

Chemistry. ^{1}H NMR spectra: Bruker AM-400 (400 MHz) instrument (Rheinstetten, Karlsruhe, Germany); chemical shifts δ in ppm with Me_4Si as internal standard (s, singlet; d, doublet; t, triplet; m, multiplet; br, broad), coupling constants J in Hz. EIMS: Finnignan MAT-95 mass spectrometer (Bremen, Germany), direct inlet 70 ev. ESIMS: Bruker Esquire 3000 Plus spectrometer (Billerica, MA). TLC: Precoated silica-gel 60 F_{254} plates (20 cm × 20 cm, 0.5 mm thickness) (Merck, Darmstadt, Germany); detection by UV light (254 nm). Column chromatography: silica gel (200−300 mesh; Qingdao Ocean Chemical Plant, Qingdao, China), Sephadex LH-20 (Amersham Pharmacia Biotech, San Francisco, CA). All reactions were carried out in oven or flame-dried glassware with magnetic stirring. Agilent Zorbax SB-C_{18} (4.6 mm × 250 mm, 5 μm) was utilized as analytical column, MeOH−H_2O (80:20, v/v) was adopted as mobile phase, and the UV detector was set at 350 nm with a column temperature of 30 °C. The purity of the test compounds was measured by normalization of the peak area in HPLC. Solvents were purified by standard procedures. Yields refer to chromatographical and spectroscopic homogeneous materials unless otherwise stated.

General Procedure for the Synthesis of Compounds (±)-1a−f. To a solution of silybin (100 mg, 0.2 mmol, see Supporting Information). K_2CO_3 (50 mg), and KI (10 mg) in dry DMF (5 mL) was added the appropriate 2-bromoacetamides **7** (0.4 mmol) in absolute THF (3 mL) under argon. The reaction mixture was stirred at 45 °C for 12 h. Then the mixture was poured into water (10 mL) and extracted with $CHCl_3$ (5 × 8 mL). The organic phase was separated and washed with brine (2 × 10 mL), dried over Na_2SO_4, and evaporated under reduced pressure. The residue was then column chromatographed over repeated silica gel and Sephadex LH-20 to afford (±)-**1a**−**f**.

***N*,*N*-Diethyl-2-{2-[3-(4-diethylcarbamoylmethoxy-3-methoxy-phenyl)-2-hydroxylmethyl-2,3-dihydro-benzo[1,4]dioxin-6-yl]-3,5-dihydroxy-4-oxo-4*H*-chromen-7-yloxy}-acetamide ((±)-1a).** This compound was prepared by the general method with silybin and 2-bromo-*N*,*N*-diethyl-acetamide (97 mg, 0.5 mmol) as starting materials and purified on silica gel chromatography using $CHCl_3$/MeOH (40:1) as eluent. Final major product (±)-**1a** was purified over Sephadex LH-20 column using $CHCl_3$/MeOH (80:3) as eluent. Yield: 40 mg (27%), yellow solid, HPLC purity 96.63%. ^{1}H NMR (400 MHz, Me_2CO-d_6) δ 12.61 (s, 1H, OH-5), 7.94−6.89 (m, 6H, ArH), 6.73 (s, 1H, H8), 6.34 (s, 1H, H6), 5.02 (d, 1H, J = 8.0 Hz, H11), 4.96 (s, 2H, OCH_2C=O), 4.94 (s, 2H, OCH_2C=O), 4.25 (m, 1H, H10), 3.88 (s, 3H, OCH_3), 3.79 (m, 1H, H23a), 3.53 (m, 1H, H23b), 3.44 (q, 2H, J = 7.2 Hz, CH_2CH_3), 3.42 (q, 2H, J = 7.2 Hz, CH_2CH_3), 3.37 (q, 2H, J = 7.2 Hz, CH_2CH_3), 3.32 (q, 2H, J = 7.2 Hz, CH_2CH_3), 1.22 (t, 3H, J = 7.2 Hz, CH_2CH_3), 1.17 (t, 3H, J = 7.2 Hz, CH_2CH_3), 1.06 (t, 3H, J = 7.2 Hz, CH_2CH_3), 1.02 (t, 3H, J = 7.2 Hz, CH_2CH_3). ^{13}C NMR (100 MHz, Me_2CO-d_6) δ 167.0 (*O*=CN), 166.2 (*O*=CN), 165.4 (C7), 162.4 (C5), 157.3 (C8a), 155.8 (C20), 148.5 (C19), 148.1 (C16a), 147.2 (C2), 144.6 (C12a), 138.2 (C3), 128.7 (C17), 124.0 (C14), 123.7 (C22), 121.6 (C15), 118.2 (C13), 117.6 (C16), 115.7 (C21), 111.9 (C18), 106.5 (C4a), 99.1 (C6), 93.7 (C8), 79.9 (C10), 77.1 (C11), 70.2 (OCH_2CO), 67.5 (OCH_2CO), 61.6 (C23), 56.2 (OCH_3), 40.7 (NCH_2CH_3), 40.6 (NCH_2CH_3), 40.5 (NCH_2CH_3), 40.4 (NCH_2CH_3), 14.5 (NCH_2CH_3), 13.1 (NCH_2CH_3). MS (ESI^+) m/z 707 $(M + H)^+$. MS (EI) m/z 707, 706, 634, 615, 606, 596, 548, 324, 266.

3,5-Dihydroxy-2-{2-hydroxymethyl-3-[3-methoxy-4-(2-oxo-2-pyrrolidin-1-yl-ethoxy)-phenyl]-2,3-dihydro-benzo[1,4]dioxin-6-yl}-7-(2-oxo-2-pyrrolidin-1-yl-ethoxy)-chromen-4-one ((±)-1b). This compound was prepared by the general method with silybin and 1-(bromoacetyl)-pyrrolidine (96 mg, 0.5 mmol) as starting materials and purified on silica gel chromatography using $CHCl_3$/MeOH (40:1) as eluent. Final major product (±)-**1b** was purified over Sephadex LH-20 column using $CHCl_3$/MeOH (80:3) as eluent. Yellow solid, yield: 34 mg (23%), HPLC purity 97.45%. ^{1}H NMR (400 MHz, Me_2CO-d_6) δ 12.05 (s, 1H, OH-5), 7.13−6.86 (m, 6H, ArH), 6.72 (d, 1H, J = 2.0 Hz, H8), 6.30 (d, 1H, J = 2.0 Hz, H6), 5.00 (d, 1H, J = 8.0 Hz, H11), 4.95 (s, 2H, OCH_2C=O), 4.93 (s, 2H, OCH_2C=O), 4.20 (m, 1H, H10), 3.86 (s, 3H, OCH_3), 3.75 (m, 1H, H23a), 3.47−3.44 (m, 9H, NCH_2CH_2, H23b), 1.53 (m, 8H, NCH_2CH_2). MS (ESI^-) m/z 701 $(M - H)^+$.

***N*-(4-Methoxy-phenyl)-2-[3,5-dihydroxy-2-(2-hydroxymethyl-3-{3-methoxy-4-[(4-methoxy-phenylcarbamoyl)-methoxy]-phenyl}-2,3-dihydro-benzo[1,4]dioxin-6-yl)-4-oxo-4*H*-chromen-7-yloxy]-acetamide ((±)-1c).** This compound was prepared by the general method with silybin and 2-bromo-*N*-(4-methoxy phenyl)-acetamide (146.0 mg, 0.5 mmol) as starting materials and purified on silica gel chromatography using $CHCl_3$/MeOH (40:1) as eluent. Final major product (±)-**1c** was purified over Sephadex LH-20 column using $CHCl_3$/MeOH (80:3) as eluent. Yellow solid, yield: 47 mg (28%), HPLC purity 97.02%. ^{1}H NMR (400 MHz, DMSO-d_6) δ 12.38 (s, 1H, OH-5), 7.13−6.86 (m, 14H, ArH), 7.02 (d, 1H, J = 2.0 Hz, H8), 6.51 (d, 1H, J = 2.0 Hz, H6), 4.95 (d, 1H, J = 8.0 Hz, H11), 4.80 (s, 2H, OCH_2C=O), 4.62 (s, 2H, OCH_2C=O), 4.27 (m, 1H, H10), 3.77 (s, 3H, OCH_3), 3.75 (s, 6H, OCH_3), 3.59 (m, 1H, H23a), 3.40 (m, 1H, H23b). MS (ESI^-) m/z 805 $(M - H)^+$.

***N*-(4-Chloro-phenyl)-2-[2-(3-{4-[(4-chloro-phenylcarbamoyl)-methoxy]-3-methoxy-phenyl}- 2-hydroxymethyl-2,3-dihydro-benzo[1,4]dioxin-6-yl)-3,5-dihydroxy-4-oxo-4*H*-chromen-7-yloxy]-acetamide ((±)-1d).** This compound was prepared by the general method with silybin and 2-bromo-*N*-(4-chlorophenyl)-acetamide (124 mg, 0.5 mmol) as starting materials and purified on silica gel chromatography using $CHCl_3$/MeOH (40:1) as eluent. Final major product (±)-**1d** was purified over Sephadex LH-20 column using $CHCl_3$/MeOH (80:3) as eluent. Yellow solid, yield: 38 mg (22.5%), HPLC purity 96.31%. ^{1}H NMR (400 MHz, DMSO-d_6) δ 12.05 (s, 1H, OH-5), 7.77−6.80 (m, 14H, ArH), 6.98 (d, 1H, J = 2.0 Hz, H8), 6.50 (d, 1H, J = 2.0 Hz, H6), 5.01 (d, 1H, J = 8.0 Hz, H11), 4.85 (s, 2H, OCH_2C=O), 4.67 (2H, s, OCH_2C=O), 4.26 (m, 1H, H10), 3.78 (s, 3H, OCH_3), 3.58 (m, 1H, H23a), 3.40 (m, 1H, H23b). MS (ESI^-) m/z 813 $(M - H)^+$.

***N*-*p*-Tolyl-2-(3,5-Dihydroxy-2-{2-hydroxymethyl-3-[3-methoxy-4-(*p*-tolylcarbamoyl-methoxy)-phenyl]-2,3-dihydro-benzo-[1,4]dioxin-6-yl}-4-oxo-4*H*-chromen-7-yloxy)-acetamide ((±)-1e).** This compound was prepared by the general method with silybin and 2-bromo-*N*-(4-methylphenyl)-acetamide (114 mg, 0.5 mmol) as starting materials and purified on silica gel chromatography using $CHCl_3$/MeOH (40:1) as eluent. Final major product (±)-**1e** was purified over Sephadex LH-20 column using $CHCl_3$/MeOH (80:3) as eluent. Yellow solid, yield: 42 mg (26%), HPLC purity 96.88%. ^{1}H NMR (400 MHz, DMSO-d_6) δ 12.40 (s, 1H, OH-5), 7.79−6.86 (m, 14H, ArH), 6.82 (br s, 1H, H8), 6.51 (br s, 1H, H6), 4.96 (d, 1H, J = 8.0 Hz, H11), 4.83 (s, 2H, OCH_2C=O), 4.65 (s, 2H, OCH_2C=O), 4.28 (m, 1H, H10), 3.78 (s, 3H, OCH_3), 3.59 (m, 1H, H23a), 3.40 (m, 1H, H23b), 2.27 (s, 6H, CH_3). MS (ESI^-) m/z 773 $(M - H)^+$.

***N*-(2,4-Dichloro-phenyl)-2-[2-(3-{4-[(2,4-dichloro-phenylcarbamoyl)-methoxy]-3-methoxy- phenyl}-2-hydroxymethyl-2,3-dihydro-benzo[1,4]dioxin-6-yl)-3,5-dihydroxy-4-oxo-4*H*-chromen-7-yloxy]-acetamide [(±)-1f].** This compound was prepared by the general method with silybin and 2-bromo- *N*-(2,4-dichlorophenyl)-acetamide (142.0 mg, 0.5 mmol) as starting materials and purified on silica gel chromatography using $CHCl_3$/MeOH (30:1) as eluent. Final major product (±)-**1f** was purified over Sephadex LH-20 column using $CHCl_3$/MeOH (80:3) as eluent. Yellow solid, yield: 47 mg (29%), HPLC purity 95.53%. ^{1}H NMR (400 MHz, DMSO-d_6) δ 12.40 (s, 1H, OH-5),

7.64−6.90 (m, 12H, ArH), 7.00 (d, 1H, J = 2.0 Hz, H8), 6.52 (d, 1H, J = 2.0 Hz, H6), 4.96 (d, 1H, J = 8.0 Hz, H11), 4.83 (s, 2H, OCH_2C=O), 4.65 (s, 2H, OCH_2C=O), 4.28 (m, 1H, H10), 3.78 (s, 3H, OCH_3), 3.59 (m, 1H, H23a), 3.40 (m, 1H, H23b). MS (ESI^-) m/z 881 $(M - H)^+$.

Preparation of 7−OH Monoether 2. *N*,*N*-Diethyl-2-{2-[3-(3-methoxy-4- hydroxyphenyl)-2-hydroxylmethyl-2,3-dihydro-benzo[1,4]dioxin-6-yl]-3,5-dihydroxy-4-oxo-4*H*-chromen-7-yloxy}-acetamide ((±)-2). This compound was prepared by the general method with silybin and 2-bromo-*N*,*N*-diethyl-acetamide (40 mg, 0.2 mmol) as starting materials and purified on silica gel chromatography using $CHCl_3$/MeOH (40:1) as eluent. Final major product (±)-**2** was purified over Sephadex LH-20 column using $CHCl_3$/MeOH (80:3) as eluent. Yield: 25 mg (20%), yellow solid, HPLC purity 97.71%. ^{1}H NMR (400 MHz, Me_2CO-d_6) δ 12.58 (1H, s, OH-5), 7.89−6.78 (m, 6H, ArH), 6.72 (br s, 1H, H8), 6.33 (br s, 1H, H6), 5.00 (d, 1H, J = 8.0 Hz, H11), 4.93 (s, 2H, OCH_2C=O), 4.24 (m, 1H, H10), 3.78 (m, 1H, H23a), 3.76 (s, 3H, OCH_3), 3.56 (m, 1H, H23b), 3.42 (q, 2H, J = 7.2 Hz, OCH_2CH_3), 3.38 (q, 2H, J = 7.2 Hz, OCH_2CH_3), 1.22 (t, 3H, J = 7.2 Hz, OCH_2CH_3), 1.18 (t, 3H, J = 7.2 Hz, OCH_2CH_3). MS (ESI^+) m/z 594 $(M + H)^+$.

Preparation of 2-[3-(4-Ethoxycarbonylmethoxy-3-methoxy-phenyl)-2-hydroxylmethyl-2,3-dihydro-benzo[1,4]dioxin-6-yl]-3,-5-dihydroxy-4-oxo-4*H*-chromen-7-yloxy-acetyl Ethyl Ester ((±)-3). To a solution of silybin (48 mg, 0.1 mmol), K_2CO_3 (11 mg), and KI (2 mg) in dry DMF (6 mL) was added 22.5 mg of chloroacetic acid ethyl ester (0.4 mmol) in 1 mL of DMF under argon. The reaction mixture was stirred at 45 °C for 12 h. The cooled mixture was poured into ice−water (10.0 g). The yellowish precipitates solid was then filtrated, washed by distilled water, dried over Na_2SO_4, and subjected to a silica gel column chromatography, using PET/EtOAc (1:1) as eluent. Final major product (±)-**3** was purified over Sephadex LH-20 column using $CHCl_3$/MeOH (30:1) as eluent. Yield: 26 mg (26%), yellow solid, HPLC purity 97.27%. ^{1}H NMR (400 MHz, $CDCl_3$) δ 11.20 (1H, s, OH-5), 8.24−6.88 (m, 6H, ArH), 6.66 (br s, 1H, H8), 6.20 (br s, 1H, H6), 4.88 (d, 1H, J = 7.6 Hz, H11), 4.26 (q, 2H, J = 7.2 Hz, $COCH_2CH_3$), 4.22 (q, 2H, J = 7.2 Hz, $COCH_2CH_3$), 4.93 (s, 2H, OCH_2C=O), 4.24 (m, 1H, H10), 3.84 (m, 1H, H23a), 3.78 (s, 3H, OCH_3), 3.58 (m, 1H, H23b), 3.42 (s, 2H, $COCH_2O$), 3.39 (s, 2H, $COCH_2O$), 1.30 (t, 3H, J = 7.2 Hz, $COCH_2CH_3$), 1.28 (t, 3H, J = 7.2 Hz, $COCH_2CH_3$). MS (ESI^+) m/z 653 $(M + H)^+$.

Preparation of (±)-2-[3-(4-Ethenylmethoxy-3-methoxy-phenyl)-2-hydroxylmethyl-2,3- dihydro-benzo[1,4]dioxin-6-yl]-3,5-dihydroxy-4-oxo-4*H*-chromen-7-yloxy-allyl Ether ((±)-4a). To a solution of silybin (241 mg, 0.5 mmol), 276 mg of K_2CO_3 (2.0 mmol) in 5 mL of dry DMF was added 150 mg of allyl bromide dropwise under argon. The reaction mixture was stirred at 55 °C for 3 h. The cooled mixture was poured into ice−water (20 g) and extracted with EtOAc (3 × 10 mL). The organic phase was separated and washed with brine (2 × 10 mL), dried over Na_2SO_4, and evaporated under reduced pressure. The yellowish residue was subjected to a column chromatography over silica gel, using $CHCl_3$/EtOAc/AcOH (20:1:0.1) as eluent. Final major product (±)-**4a** was purified over Sephadex LH-20 column using $CHCl_3$/MeOH (80:3) as eluent. Yield: 77 mg, (27%), yellowish solid, HPLC purity 95.84%. ^{1}H NMR (400 MHz, Me_2CO-d_6) δ 11.65 (1H, s, O*H*-5), 7.12−6.68 (6H, m, ArH), 6.17 (1H, br s, H8), 6.11 (1H, br s, H6), 6.06 (1H, m, OCH_2CH=CH_2), 6.02 (1H, m, OCH_2CH=CH_2), 5.28−5.06 (4H, m, OCH_2CH=CH_2), 4.92 (1H, d, J = 7.6 Hz, H11), 4.26−4.21 (4H, m, OCH_2CH=CH_2), 4.21 (1H, m, H10), 3.89 (1H, m, H23a), 3.78 (3H, s, OCH_3), 3.63 (1H, m, H23b). MS (ESI^+) m/z 561 $(M + H)^+$.

Preparation of (±)-2-[3-(4-Allylmethoxy-3-methoxy-phenyl)-2-hydroxylmethyl-2,3-dihydro-benzo[1,4]dioxin-6-yl]-3,5-dihydroxy-4-oxo-4*H*-chromen-7-yloxy-butenyl Ether ((±)-4b). To a solution of silybin (241 mg, 0.5 mmol) and 276 mg of K_2CO_3 (2.0 mmol) in 5 mL of dry DMF was added 150.0 mg (1.11 mmol) of butenyl bromide dropwise under argon. The reaction mixture was stirred at 55 °C for 3 h. The cooled mixture was poured into ice−water (20 g) and worked up as above. The yellowish residue was subjected to a column chromatography over 10.0 g silica gel, using $CHCl_3$/EtOAc/AcOH (20:1:0.1) as eluent (R_f 0.45). Final major product (±)-**4b** was purified over Sephadex LH-20 column using $CHCl_3$/MeOH (80:3) as eluent. Yield: 32 mg (11%), yellowish solid, HPLC purity 95.13%. ^{1}H NMR (400 MHz, $CDCl_3$) δ 12.64 (s, 1H, 5−OH), 7.77 (d, J = 1.6 Hz, 1H, H18), 7.76 (d, J = 1.6 Hz, 1H, H13), 7.08 (d, 1H, J = 8.8 Hz, H21), 7.00 (br d, 1H, J = 8.8 Hz, H22), 6.98 (br d, 1H, J = 8.4 Hz, H15), 6.94 (d, 1H, J = 8.4 Hz, H16), 6.41 (d, 1H, J = 2.0 Hz, H8), 6.34 (d, 1H, J = 2.2 Hz, H6), 5.78−5.92 (m, 2H, H3′,3″), 5.05−5.21 (m, 4H, H4′,4″), 5.02 (d, 1H, J = 8.2 Hz, H11), 4.05−4.15 (m, 5H, H1′,1″,10), 3.95 (s, 3H, OCH_3), 3.88 (m, 1H, H23b), 3.61 (br dd, 1H, J = 8.8, 3.2 Hz, H23a), 2.50−2.65 (m, 4H, H2′,2″). ^{13}C NMR (100 MHz, $CDCl_3$) δ 178.77 (C, C4), 164.67 (C, C7), 161.85 (C, C5), 156.63 (C, C8a), 155.45 (C, C2), 146.89 (C, C19), 146.43 (C, C12a), 145.59 (C, C16a), 143.60 (C, C20), 138.12 (C, C3), 134.43 (CH, C3″), 133.7 (CH, C3′), 127.50 (C, C17), 123.84 (C, C14), 122.76 (CH, C22), 120.75 (CH, C15), 117.50 (CH, C21), 117.27 (CH, C16), 117.06 (CH_2, C4″), 116.97 (CH_2, C4′), 114.68 (CH, C18), 109.37 (CH, C13), 105.93 (C, C4a), 98.24 (CH, C6), 92.44 (CH, C8), 78.67 (CH, C10), 76.28 (CH, C11), 71.88 (CH_2, C1″), 67.66 (CH_2, C1′), 61.55 (CH_2, C23), 55.98 (OCH_3), 34.46 (CH_2, C2″), 33.20 (CH_2, C2′). MS (ESI^+) m/z 589 $(M + H)^+$.

Preparation of (±)-2-[3-(4-Isopentenyloxy-3-methoxy-phenyl)-2-hydroxylmethyl-2,3-dihydro-benzo[1,4]dioxin-6-yl]-3,5-dihydroxy-4-oxo-4*H*-chromen-7-yloxy-isopentenyl Ether ((±)-4c). To a solution of silybin (241 mg, 0.5 mmol) and 276 mg of K_2CO_3 (2.0 mmol) in 5 mL of dry DMF was added 165.0 mg (1.11 mmol) of isopentenyl bromide dropwise under argon. The reaction mixture was stirred at 75 °C for 3 h. The cooled mixture was poured into ice−water (20 g) and worked up as above. The yellowish residue was subjected to a column chromatography over 10.0 g silica gel, using $CHCl_3$/EtOAc/AcOH (7:1:0.1) as eluent (R_f 0.49). Final major product (±)-**4c** was purified over Sephadex LH-20 column using $CHCl_3$/MeOH (30:1) as eluent. Yield: 49 mg (16%), yellowish solid, HPLC purity 96.69%. ^{1}H NMR (400 MHz, $CDCl_3$) δ 12.69 (s, 1H, 5−OH), 7.79 (d, 1H, J = 8.0 Hz, H15), 7.75 (br s, 1H, H13), 7.08 (d, 1H, J = 8.8 Hz, H21), 6.92−7.01 (m, 3H, ArH16,18,22), 6.42 (br s, 1H, H8), 6.35 (d, 1H, J = 1.6 Hz, H6), 5.44−5.53 (m, 2H, H2′,2″), 5.02 (d, 1H, J = 8.0 Hz, H11), 4.55−4.63 (m, 4H, H1′,1″), 4.15 (m, 1H, H10), 3.85 (s, 3H, OCH_3), 3.75 (m, 1H, H23b), 3.60 (m, 1H, H23a), 1.81 (s, 3H, CH_3), 1.79 (s, 3H, CH_3), 1.75 (s, 6H, 2 CH_3). MS (ESI^+) m/z 617 $(M + H)^+$.

Preparation of (±)-2-[3-(4-Ethenylmethoxy-3-methoxy-phenyl)-2-hydroxylmethyl-2,3- dihydro-benzo[1,4]dioxin-6-yl]-3-allyloxy-5-hydroxy-4-oxo-4*H*-chromen-7-yloxy-allyl ether ((±)-4d). To a solution of silybin (241 mg, 0.5 mmol) and 276 mg of K_2CO_3 (2.0 mmol) in 5 mL of dry DMF was added 200.0 mg (1.65 mmol) of allyl bromide dropwise under argon. The reaction mixture was stirred at 75 °C for 3 h. The cooled mixture was poured into ice−water (20 g) and worked up as above. The yellowish residue was subjected to a column chromatography, using petroleum ether/EtOAc (6:1) as eluent (R_f 0.33), over 10.0 g silica gel. Final major product (±)-**4d** was purified over Sephadex LH-20 column using $CHCl_3$/MeOH (80:3) as eluent. Yield: 40 mg (13%), yellowish solid, HPLC purity 95.55%. ^{1}H NMR (400 MHz, Me_2CO-d_6) δ 12.70 (s, 1H, 5−OH), 7.82 (dd, 1H, J = 8.8, 2.0 Hz, H15), 7.75 (d, 1H, J = 2.0 Hz, H13), 7.19 (d, 1H, J = 8.0 Hz, H18), 7.03−7.10 (m, 3H, ArH16,21,22), 6.77 (d, 1H, J = 2.0 Hz, H8), 6.35 (d, 1H, J = 2.0 Hz, H−6), 6.10 (m, 3H, H−2′,2″,2‴), 5.17−5.48 (m, 6H, H−3′,3″,3‴), 5.10 (d, 1H, J = 8.0 Hz, H11), 4.72 (d, 2H, J = 5.2 Hz, H1‴), 4.67 (d, 2H, J = 6.0 Hz, H1″), 4.62 (d, 2H, J = 5.2 Hz, H1′), 4.27 (m, 1H, H10), 3.87 (s, 3H, OCH_3), 3.54 (m, 2H, H23). MS (ESI^+) m/z 601 $(M + H)^+$.

Preparation of (±)-2-[3-(4-Allylmethoxy-3-methoxy-phenyl)-2-hydroxylmethyl-2,3-dihydro-benzo[1,4]dioxin-6-yl]-3-buteny-loxy-5-hydroxy-4-oxo-4*H*-chromen-7-yloxy-butenyl ether ((±)-4e). To a solution of silybin (241 mg, 0.5 mmol) and 276 mg of K_2CO_3 (2.0 mmol) in 5 mL of dry DMF was added 222 mg of butenyl bromide dropwise under argon. The reaction mixture was stirred at 75 °C for 3 h. The cooled mixture was poured into ice−water (20 g) and worked up as above. The yellowish residue was subjected to a column chromatography, using $CHCl_3$/EtOAc/AcOH (20:1:0.5) as eluent over 10.0 g silica gel (R_f 0.50). Final major product (±)-**4e** was purified over Sephadex LH-20 column using $CHCl_3$/MeOH (40:1) as eluent. Yield: 33 mg (10%), yellowish solid, HPLC purity 96.52%. ^{1}H NMR (400 MHz, $CDCl_3$) δ 12.63 (s, 1H, 5−OH), 7.09 (d, 1H, J = 8.8 Hz, H15), 7.78 (br s, 2H, H13,18), 7.09 (d, 1H, J = 8.8 Hz, H21), 7.02 (br d, 1H, J = 8.0 Hz, H22), 6.97 (br d, 1H, J = 8.0 Hz, H15), 6.94 (d, 1H, J = 8.4 Hz, H16), 6.42 (d, 1H, J = 2.0 Hz, H8), 6.34 (d, 1H, J = 2.0 Hz, H6), 5.79−5.98 (m, 3H, H3′,3″,3‴), 5.08−5.22 (m, 6H, H4′,4″,4‴), 5.03 (d, 1H, J = 8.4 Hz, H11), 4.05−4.16 (m, 7H, H1′,1″,1‴,10), 3.91 (s, 3H, OCH_3), 3.75 (m, 1H, H23b), 3.59 (m, 1H, H23a), 2.43−2.67 (m, 6H, H2′,2″,2‴). ^{13}C NMR (100 MHz, $CDCl_3$) δ 178.77 (C, C4), 164.66 (C, C7), 161.85 (C, C5), 156.63 (C, C8a), 155.44 (C, C2), 149.75 (C, C19), 149.02 (C, C12a), 145.59 (C, C16a), 143.60 (C, C20), 134.43 (CH, C3″), 138.13 (C, C3), 133.7 (CH, C3′), 133.95 (CH, C3‴), 128.23 (C, C17), 123.85 (C, C14), 122.78 (CH, C22), 120.07 (CH, C15), 117.62 (CH_2, C4‴), 117.51 (CH, C21), 117.34 (CH, C16), 117.07 (CH_2, C4″), 116.97 (CH_2, C4′), 112.94 (CH, C18), 110.40 (CH, C13), 105.93 (C, C4a), 98.24 (CH, C6), 92.44 (CH, C8), 78.63 (CH, C10), 76.20 (CH, C11), 71.88 (CH_2, C1″), 68.19 (CH_2, C1‴), 67.66 (CH_2, C1′), 61.55 (CH_2, C23), 56.07 (OCH_3), 34.48 (CH_2, C−2‴), 33.48 (CH_2, C−2″), 33.20 (CH_2, C−2′). MS (ESI^+) m/z 643 $(M + H)^+$.

Preparation of (±)-2-[3-(4-Hydroxy-3-methoxy-phenyl)-2-hydroxylmethyl-2,3-dihydro-benzo[1,4]dioxin-6-yl]-3,5-dihydroxy-4-oxo-4*H*-chromen-7-yloxy-isopentenyl Ether ((±)-4f). To a solution of silybin (241 mg, 0.5 mmol) and 276 mg of K_2CO_3 (2.0 mmol) in 5 mL of dry DMF was added 75 mg (0.5 mmol) of isopentenyl bromide dropwise under argon. The reaction mixture was stirred at 55 °C for 1 h. The cooled mixture was poured into ice−water (20 g) and worked up as above. The yellowish residue was subjected to a column chromatography, using petroleum ether/EtOAc/AcOH (5:1:0.1) as eluent (R_f 0.34), over 10.0 g silica gel. Final major product (±)-**4f** was purified over Sephadex LH-20 column using $CHCl_3$/MeOH (30:1) as eluent. Yield: 39 mg (14%), yellowish solid, HPLC purity 96.16%. ^{1}H NMR (400 MHz, $CDCl_3$) δ 11.69 (s, 1H, 5−OH), 7.87 (s, 1H, H13), 7.82 (d, 1H, J = 8.0 Hz, H15), 7.09 (d, 1H, J = 8.4 Hz, H21), 6.98 (s, 1H, H18), 6.97 (d, 2H, J = 8.4 Hz, ArH16,22), 6.73 (s, 1H, OH), 6.45 (s, 1H, H8), 6.37 (s, 1H, H6), 5.81 (s, 1H, OH), 5.48 (m, 1H, H2′), 5.01 (d, 1H, J = 8.4 Hz, H11), 4.57 (d, 2H, J = 6.4 Hz, H1′), 4.12 (m, 1H, H10), 3.93 (s, 3H, OCH_3), 3.75 (m, 1H, H23b), 3.60 (m, 1H, H23a), 1.81 (s, 3H, 4′CH_3), 1.76 (s, 3H, 5′CH_3). MS (ESI^+) m/z 549 $(M + H)^+$.

General Procedure for the Synthesis of Compounds (±)-5a and (±)-5b. To a solution of silybin (100.0 mg, 0.2 mmol), TPP (160 mg, 0.57 mmol) and DEAD (100 mg, 0.57 mmol) in absolute THF (10 mL) was added the appropriate acid (0.4 mmol) in absolute THF (3 mL) under argon. The reaction mixture was stirred at 60 °C for 10 h. Then the mixture was concentrated in vacuo. The residue was poured into water and extracted with $CHCl_3$ (3×10 mL). The organic phase was separated and washed with brine, dried over Na_2SO_4, and evaporated under reduced pressure to give yellow oil. The oil was chromatographed on repeated silica gel and Sephadex LH-20 columns to afford (±)-**5a**−**b**.

4-Methoxy Benzoic Acid, Mono[[2,3-dihydro-3-(4-hydroxy-3-methoxyphenyl)-6-(3,5,7-trihydroxy-4-oxo-4*H*-1-benzopyran-2-yl)-1,4-benzodioxin-2-yl] methyl] Ester ((±)-5a). This compound was prepared by the general method with silybin and 4-methoxybenzoic acid (61 mg) as starting materials and purified on silica gel chromatography using $CDCl_3$/AcOEt (50:1) as eluent. Final major product (±)-**5a** was purified over Sephadex LH-20 column using $CHCl_3$/MeOH (40:1) as eluent. Yield: 29 mg (22.5%), yellow solid, HPLC purity 96.07%. ^{1}H NMR (400 MHz, $CDCl_3$) δ 11.15 (s, 1H, OH-5), 7.99−6.83 (m, 10H, ArH), 6.14 (br s, 1H, H8), 6.10 (br s, 1H, H6), 5.00 (d, 1H, J = 8.0 Hz, H11), 4.48 (m, 1H, H23a), 4.28 (m, 1H, H10), 4.27 (m, 1H, H23b), 3.86 (s, 3H, OCH_3), 3.80 (s, 3H, OCH_3). ^{13}C NMR (100 MHz, $CDCl_3$) δ 175.6 (C4), 166.0 (C1′), 164.2 (C7), 162.8 (C5′), 161.2 (C5), 157.4 (C8a), 148.1 (C16a), 147.4 (C19), 147.2 (C20), 146.5 (C2), 144.3 (C12a), 137.3 (C3), 130.9 (C3′, C7′), 126.9 (C17), 123.6 (C14), 121.5 (C15), 121.2 (C2′), 120.6 (C22), 117.3 (C13), 116.8 (C16), 115.1 (C21), 113.6 (C4′, C6′), 111.8 (C18), 107.4 (C4a), 99.4 (C6), 93.8 (C8), 79.1 (C10), 77.0 (C11), 64.8 (C23), 56.8 (OCH_3), 56.6 (OCH_3). MS (ESI^-) m/z 613 $(M - H)^+$.

3-Chlorobenzoic Acid, Mono[[2,3-dihydro-3-(4-hydroxy-3-methoxyphenyl)-6-(2,3-dihydro- 3,5,7-trihydroxy-4-oxo-4*H*-1-benzopyran-2-yl)-1,4-benzodioxin-2-yl]methyl] Ester ((±)-5b). This compound was prepared by the general method with silybin and 3-chlorobenzoic acid (62 mg, 0.4 mmol) as starting materials and purified on silica gel chromatography using $CDCl_3$/AcOEt (50:1) as eluent. Final major product (±)-**1a** was purified over Sephadex LH-20 column using $CHCl_3$/MeOH (40:1) as eluent. Yield: 29 mg (23%), yellow solid, HPLC purity 97.27%. ^{1}H NMR (400 MHz, $CDCl_3$) δ 11.08 (s, 1H, OH-5), 7.96−6.82 (m, 11H, ArH), 6.11 (br s, 1H, H8), 6.08 (br s, 1H, H6), 5.01 (d, 1H, J = 8.0 Hz, H11), 4.55 (m, 1H, H23a), 4.39 (m, 1H, H10), 4.20 (m, 1H, H23b), 3.81 (s, 3H, OCH_3). ^{13}C NMR (100 MHz, $CDCl_3$) δ 175.6 (C4), 166.9 (C1′), 164.9 (C7), 1618 (C5), 157.8 (C8a), 148.0 (C16a), 147.3 (C19), 146.9 (C20), 146.1 (C2), 144.5 (C12a), 137.5 (C3), 133.9 (C4′), 133.3 (C5′), 131.7 (C2′), 130.2 (C3′), 129.6 (C6′), 127.9 (C7′), 127.7 (C17), 123.3 (C14), 121.7 (C15), 120.5 (C22), 116.7 (C13), 116.9 (C16), 115.3 (C21), 111.2 (C18), 107.7 (C4a), 99.5 (C6), 93.7 (C8), 79.1 (C10), 77.1 (C11), 65.2 (C23), 55.9 (OCH_3). MS (ESI^-) m/z 617 $(M - H)^+$.

DPPH Free Radical Scavenging Activity. Quenching of free radicals by the synthesized compounds was assayed spectrophotometrically at 517 nm against the absorbance of the stable radical DPPH.[105] The effect of test compounds on free radical scavenging was reflected by the decolorization monitored of DPPH radical. In brief, reaction mixtures dissolved in methanol containing various concentrations of the test compounds dissolved in DMSO and DPPH (0.4 mg/mL). The methanolic solution of DPPH served as a control while quercetin, vitamin C, silybin, and DHS were used as reference free radical scavengers. The absorbance was measured at 517 nm on an ELISA plate reader after the mixture was incubated at 37 °C for 30 min.

Superoxide Anion Scavenging Activity. The superoxide anion scavenging activities of synthesized compounds were assayed spectrophotometrically as previously reported with slight modification.[106] Superoxide anion radicals were generated in a nonenzymic phenazine methosulfate−NADH system by following of the reduction of nitroblue tetrazolium. In this assay, the superoxide anion radicals were measured in plates, which contained 78 μM of NADH, 50 μM of nitroblue tetrazolium, 5 μM of phenazine methosulfate and the tested samples with different concentrations in 16 mM Tris-HCl buffer at pH 8.0. The luminosity was monitored at 560 nm after 5 min of incubation at room temperature. The blank samples did not contain phenazine methosulphate. Quercetin, vitamin C, silybin, and DHS were used as reference inhibitors.

Inhibition of LPO by the TBARS Assay on Rat Liver Homogenates. As an indicator of the levels of lipid peroxidation, formation of malondialdehyde (MDA) was examined by the thiobarbituric acid reactive substances (TBARS) assay on rat liver homogenates in ice-cold PBS, using colorimetry.[70,107,108] The livers were promptly removed from euthanized male Spwague−Dawley rats, and then homogenized with 4 °C normal

saline by a glass homogenizer to produce 5% liver homogenates−normal saline solution. The reaction mixtures which composed of 200 μL of solution containing an aqueous $FeSO_4$ (4 μM), vitamin C (50 μM), 50 μL of freshly prepared rat liver homogenates, and 5 μL of the test compounds (concentrations from 0.02 to 200 μM), were incubated at 37 °C in capped tubes for 1 h before 100 μL of trichloroacetic acid (20%, v/v) was added. The mixture reacted at room temperature for 30 min. Finally, 200 μL of HCl (0.1 M) and 100 μL of TBA (1%, v/v) were added into each tube and the mixture was incubated at 100 °C for another 1 h. Centrifugation was then carried out at 2000*g* for 5 min, and the absorbance of the supernatant was measured at 532 nm, quercetin, silybin, and DHS were served as the positive standards.

Ferrous Ion Chelation Measurement. The ferrous ion chelation by the test compounds were determined by the reported method.[109] Briefly, the samples with final concentrations ranging from 1 to 200 μM were added to a solution of 2 mM $FeSO_4$ (5 μL) and 80% DMSO (200 μL). The reaction was initiated by adding 5 mM ferrozine (10 μL), and the mixture was shaken vigorously before left standing at room temperature for 10 min. The absorbance of the solution was measured spectrophotometrically at 562 nm. The percentage inhibition of ferrozine−Fe^{2+} complex formation was calculated as $[(A_0 - A_1)/A_0] \times 100$, where A_0 was the absorbance of the ferrozine−Fe^{2+} complex, and A_1 was the absorbance in the presence of test compound. EDTA-2Na was used as the positive control, while silybin and quercetin were also introduced as reference compounds.

Protection of PC12 Cells Against H_2O_2-induced Cell Injury.[110] The rat pheochromocytoma (PC12) cells were maintained at 37 °C in a humidified atmosphere containing 5% CO_2. PC12 cells were seeded into multiwell plates (96) at a density of 6×10^3 per well in DMEM (high sucrose), supplemented with 10% heat-inactivated bovine calf serum, 100 units/mL penicillin, and 100 units/mL of streptomycin. All experiments were carried out 36 h after cells were seeded. The PC12 cells were preincubated with samples, which were dissolved in DMSO and diluted with medium to the final concentrations of 12.5, 25, and 50 μM, respectively. After 2 h, H_2O_2 (diluted with 0.9% NaCl solution to a final concentration of 500 μM) was added. Assays for cell viability were performed 4 h after H_2O_2 was added. Cell survivals were evaluated by two methods: morphological observation with phase-contrast microscope and MTT assay. A fresh solution of MTT (5 mg/mL) prepared in NaCl (0.9%) solution was added to each well, and the plates were incubated in a CO_2 incubator at 37 °C for an additional 3 h. The MTT solution was aspirated off and then 200 μL of DMSO was added to each well to solubilize the formazan crystals in viable cells. The absorbance was measured at 570 nm. Compared with the normal cells, the viability of cells treated with drugs is calculated by the following formula: OD (drug-treated)/OD (normal cells) × 100%, while the negative control is calculated as OD (DMSO, which is used to exclude the effective of solvent on the result)/OD (normal cells) × 100%. Thus the increased cell viability could be calculated as [OD (drug-treated)/OD (normal cells) × 100%] − [OD (DMSO)/OD (normal cells) × 100%]. Silybin, DHS, and quercetin served as the positive standards.

Inhibition Assay of Xanthine Oxidase. The XO activity was evaluated by the spectrophotometric measurement of the formation of formazan.[111,112] The reaction mixture in the sample wells consisted of xanthine oxidase (600 μL, 540 μM final concentration) obtained from rat liver, in phosphate buffer 0.01 M, pH 8.75 (30 μL), NBT (30 μL, 100 μM, final concentration), PMS (30 μL, 100 μM final concentration), Triton X-100 (10 μL, 0.4%), and the test compounds (30 μL, at an original concentration of 75 μM). After 2 h of incubation at 37 °C in water bath, the color was read at 550 nm. Xanthine was omitted in the blank samples. Allopurinol was used as positive control, while silybin and DHS were also measured as reference compounds in the assay.

Acknowledgment. This work is supported partially by the intramural foundation from Wenzhou Medical College and Zhejiang University. The authors thank Zhejiang Hisun Pharmaceutical Co. Ltd. for affording some instrumental assistance. We thank Professor Joachim Stöckigt from the University of Mainz and Professor Lihe Zhang (Beijing University) for useful discussions and encouragement on this research topic. Professor Dannel Ferreira also afforded some kind comments for this paper. We are in debt to Professor Christopher H. K. Cheng (CHKU) for his critical reading of the manuscript.

Supporting Information Available: Total synthesis process and the ^1H, ^{13}C NMR spectra and MS data of intermediates **8**−**13**, (±)-taxifolin, (±)-silybin, and (±)-isosilybin. This material is available free of charge via the Internet at http://pubs.acs.org.

References

(1) Lin, M. T; Beal, M. F. Mitochondrial dysfunction and oxidative stress in neurodegenerative diseases. *Nature* **2006**, *443*, 787–795.
(2) Goedert, M.; Spillantini, M. G. A century of Alzheimer's disease. *Science* **2006**, *314*, 777–781.
(3) Jiang, X.; Ao, L.; Zhou, C.; Yang, L.; Zhang, Q.; Li, H.; Sun, L.; Wu, X.; Bai, H.; Zhao, Y. Design, synthesis, and evaluation of two series of territrem B analogues. *Chem. Biodiversity* **2005**, *2*, 557–567.
(4) Zhao, J.; Zhao, F.; Wang, Y.; Li, H.; Zhang, Q.; Guénard, D.; Ge, Q.; Wei, E.; Jiang, H.; Wu, Y.; Wang, L.; Jiang, H.; Guéritte, F.; Wu, X.; Cheng, C. H. K.; Lee, S.-S.; Zhao, Y. Synthesis of A/B ring analogs of territrem B and evaluation of their biological activities. *Helv. Chim. Acta* **2004**, *87*, 1832–1853.
(5) Everse, J.; Coates, P. W. Role of peroxidases in Parkinson disease: a hypothesis. *Free Radical Biol. Med.* **2005**, *38*, 1296–1310.
(6) Tuppo, E. E.; Forman, L. J. Free radical oxidative damage and Alzheimer's disease. *J. Am. Osteopath. Assoc.* **2001**, *101*, S-11–S15.
(7) Perry, G.; Cash, A. D.; Smith, M. A. Alzheimer's disease and oxidative stress. *J. Biomed. Biotechnol.* **2002**, *2*, 120–123.
(8) Halleck, M. M.; Richburg, J. H.; Kauffman, F. C. Reversible and irreversible oxidant injury to PC12 cells by hydrogen peroxide. *Free Radical Biol. Med.* **1992**, *12*, 137–144.
(9) Greene, L. A.; Tischler, A. S. Establishment of a noradrenergic clonal line of rat adrenal pheochromocytoma cells which respond to nerve growth factor. *Proc. Natl. Acad. Sci. U.S.A.* **1976**, *73*, 2424–2428.
(10) Sasaki, N.; Baba, N.; Matsuo, M. Cytotoxicity of reactive oxygen species and related agents toward undifferentiated and differentiated rat phenochromocytoma PC12 cells. *Biol. Pharm. Bull.* **2001**, *24*, 515–519.
(11) Zhang, H.-Y.; Liu, Y.-H.; Wang, H.-Q.; Xu, J.-H.; Hu, H.-T. Peurarin protects PC12 cells against β-amyloid-induced cell injury. *Cell Biol. Int.* **2008**, *32*, 1230–1237.
(12) Montiel, T.; Quiroz-Baez, R.; Massieu, L.; Arias, C. Role of oxidative stress on β-amyloid neurotoxicity elicited during impairment of energy in the hippocampus: protection by antioxidants. *Exp. Neurol.* **2006**, *200*, 496–508.
(13) Sung, Y. J.; Cheng, C. L.; Chen, C. S.; Huang, H. B.; Huang, F. L.; Wu, P. C.; Shiao, M. S.; Tsay, H. J. Distinct mechanisms account for beta-amyloid toxicity in PC12 and differentiated PC12 neuronal cells. *J. Biomed. Sci.* **2003**, *10*, 379–388.
(14) Ramassamy, C.; Averill, D.; Beffert, U.; Bastianetto, S.; Theroux, L.; Lussier-Cacan, S.; Cohn, J. S.; Christen, Y.; Davignon, J.; Quirion, R.; Poirier, J. Oxidative damage and protection by antioxidants in the frontal cortex of Alzheimer's disease is related to the apolipoprotein E genetype. *Free Radical Biol. Med.* **1999**, *27*, 544–553.
(15) Pratico, D.; Uryu, K.; Leight, S.; Trojanowski, J. Q.; Lee, V. M. Increased lipid peroxidation precedes amyloid plaque formation in an animal model of Alzheimer's amyloidosis. *Exp. Neurol.* **2001**, *21*, 4183–4187.
(16) Williams, T. I.; Lynn, B. C.; Markesbery, W. R.; Lovell, M. A. Increased levels of 4-hydroxynonenal and acrolein, neurotoxic markers of lipid peroxidation, in the brain in mild cognitive impairment and early Alzheimer's disease. *Neurobiol. Aging* **2006**, *397*, 170–173.

(17) Pharm, D. Q.; Plakogiannis, R. Vitamin E supplementation in Alzheimer's disease, Parkinson's disease, tardive dyskinesia, and cataract: part 2. *Ann. Pharmacother.* **2005**, *39*, 2065–2071.

(18) Prasad, K. N.; Cole, W. C.; Kumar, B. Multiple antioxidants in the prevention and treatment of Parkinson's disease. *J. Am. Coll. Nutr.* **1999**, *18*, 413–423.

(19) Li, F. Q.; Wang, T.; Pei, Z.; Liu, B.; Hong, J. S. Inhibition of microglial activation by the herbal flavonoid baicalein attenuates inflammation-mediated degeneration of dopaminergic neurons. *J. Neural Transm.* **2005**, *112*, 331–347.

(20) Gažák, R.; Walterová, D.; Křen, V. Silybin and silymarin—new and emerging applications in medicine. *Curr. Med. Chem.* **2007**, *14*, 315–338.

(21) Švagera, Z.; Škottová, N.; Váňa, P.; Večeřa, R.; Urbánek, K.; Belejová, M.; Kosina, P.; Šimánek, V. Plasma lipoproteins in transport of silibinin, an antioxidant flavonolignan from *Silybum marianum*. *Phytother. Res.* **2003**, *17*, 524–530.

(22) Gažák, R.; Svobodová, A.; Psotová, J.; Sedmera, P.; Přikrylová, V.; Walterová, D.; Křen, V. Oxidised derivatives of silybin and their antiradical and antioxidant activity. *Bioorg. Med. Chem.* **2004**, *12*, 5677–5687.

(23) Varga, Z.; Czompa, A.; Kakuk, G.; Antus, A. Inhibition of the superoxide anion release and hydrogen peroxide formation in PMNLs by flavonolignans. *Phytother. Res.* **2001**, *15*, 608–612.

(24) Sonnenbichler, J.; Mattersberger, J.; Machicao, F.; Rosen, H.; Zetl, I. *Flavonoids and Bioflavonoids*; Studies in Organic Chemistry, Vol. 11; Elsevier: Amsterdam, 1981; pp 458−475.

(25) Singh, R. P.; Agarwal, R. Prostate cancer prevention by silybinin. *Curr. Cancer Drug Targets* **2004**, *4*, 1–11.

(26) Zielinski, J. E. Hydrophilic and lipophilic silibinin pro-forms. U. S. patent US 6,699,900 B2, **2004**.

(27) Yang, L.; Gong, J.; Wang, F.; Zhang, Y.; Wang, Y.; Hao, X.; Wu, X.; Bai, H.; Stöckigt, J.; Zhao, Y. Synthesis and antioxidant evaluation of novel silybin analogues. *J. Enzym. Inhib. Med. Chem.* **2006**, *21*, 399–404.

(28) Huang, K. X.; Wang, F.; Yang, L. X.; Gong, J. X.; Tao, Q. F.; Zhao, Y.; Wu, X. M.; Li, X. K.; Stöckigt, J.; Qu, J. Preparation of silybin 23-esters and evaluation of their inhibitory ability against LPO and DNA protective properties. *Chin. Chem. Lett.* **2009** (in press).

(29) Kim, N. C.; Graf, T. N.; Sparacino, C. M.; Wani, M. C.; Wall, M. E. Complete isolation and characterization of silybins and isosilybins from milk thistle (*Silybum marianum*). *Org. Biomol. Chem.* **2003**, *1*, 1684–1689.

(30) Svobodová, A.; Walterová, D.; Psotová, J. Influence of silymarin and its flavonolignans on H_2O_2-induced oxidative stress in human keratinocytes and mouse fibroblasts. *Burns* **2006**, *32*, 973–979.

(31) Huber, A.; Thongphasuk, P.; Erben, G.; Lehmann, W. D.; Tuma, S.; Stremmel, W.; Chamulitrat, W. Significantly greater antioxidant anticancer activities of 2,3-dehydrosilybin than silybin. *Biochim. Biophys. Acta* **2008**, *1780*, 837–847.

(32) Thongphasuk, P.; Stremmel, W.; Chamulitrat, W. 2,3-Dehydrosilybin is a better DNA topoisomerase I inhibitor than its parental silybin. *Chemotherapy* **2009**, *55*, 42–48.

(33) Trouillas, P.; Marsal, P.; Svobodová, A.; Vostálová, J.; Gažák, R.; Hrbáč, J.; Sedmera, P.; Křen, V.; Lazzaroni, R.; Duroux, J.-L.; Walterová, D. Mechanism of the antioxidant action of silybin and 2,3-dehydrosilybin flavonolignans: a joint experimental and theoretical study. *J. Phys. Chem. A* **2008**, *112*, 1054–1063.

(34) Džubák, P.; Hajdúch, M.; Gažák, R.; Svobodová, A.; Psotová, J.; Walterová, D.; Sedmera, P.; Křen, V. New derivatives of silybin and 2,3-dehydrosilybin and their cytotoxic and P-glycoprotein modulatory activity. *Bioorg. Med. Chem.* **2006**, *14*, 3793–3810.

(35) Maitrejean, M.; Comte, G.; Barron, D.; El Kirat, K.; Conseil, G.; Di Pietro, A. The flavonolignan silybin and its hemisynthetic derivatives, a novel series of potential modulators of P-glycoprotein. *Bioorg. Med. Chem. Lett.* **2006**, *10*, 157–160.

(36) Gažák, R.; Sedmera, P.; Vrbacký, M.; Vostalova, J.; Drahota, Z.; Marhol, P.; Walterová, D.; Křen, V. Molecular mechanisms of silybin and 2,3-dehydrosilybin antiradical activity role of individual hydroxyl groups. *Free Radical Biol. Med.* **2009**, *46*, 745–758.

(37) Wang, M.-J.; Lin, W.-W.; Chen, H.-L.; Chang, Y.-H.; Ou, H.-C.; Kuo, J.-S.; Hong, J.-S.; Jeng, K.-C. G. Silymarin protects dopaminergic neurons against lipopolysaccharide-induced neurotoxicity by inhibiting microglia activation. *Eur. J. Neurosci.* **2002**, *16*, 2103–2112.

(38) Kittur, S.; Wilasrusmee, S.; Pedersen, W.; Mattson, M.; Straube-West, K.; Ward, P.; Mark, M.; Wilasrusmee, C.; Jubelt, B.; Kittur, D. S. Neurotrophic and neuroprotective effects of milk thistle (*Silybum marianum*) on neurons in culture. *J. Mol. Neurosci.* **2002**, *18*, 265–269.

(39) Mazzio, E.; Huber, J.; Darling, S.; Harris, N.; Soliman, K. F. A. Effect of antioxidants on L-glutamate and *N*-methyl-4-phenylpyridinium ion induced-neurotoxicity in PC12 cells. *Neurotoxicology* **2001**, *22*, 283–288.

(40) Nencinia, C.; Giorgia, G.; Micheli, L. Protective effect of silymarin on oxidative stress in rat brain. *Phytomedicine* **2007**, *14*, 129–135.

(41) Sakai, K.; Li, Y.; Shirakawa, T.; Kitagawa, Y.; Hirose, G. Induction of major histocompatibility complex class I modecules on human neuroblastoma line cells by a flavoid antioxidant. *Neurosci. Lett.* **2001**, *298*, 127–130.

(42) Long, K.; Boyce, M.; Lin, H.; Yuan, J.; Ma, D. Structure−activity relationship studies of salubrinal lead to its active biotinylated derivative. *Bioorg. Med. Chem.* **2005**, *15*, 3849–3852.

(43) Auvin, S.; Pignol, B.; Navet, E.; Troadec, M.; Carre, D.; Camara, J.; Bigg, D.; Chabrier, P.-E. Novel dual inhibitors of calpain and lipid peroxidation with enhanced cellular activity. *Bioorg. Med. Chem. Lett.* **2006**, *16*, 1586–1589.

(44) Taira, J.; Miyagi, C.; Aniya, Y. Dimerumic acid as an antioxidant from the mold, *Monascus anka*: the inhibition mechanisms against lipid peroxidation and hemeprotein-mediated oxidation. *Biochem. Pharmacol.* **2002**, *63*, 1019–1026.

(45) Rinderspacher, A.; Cremona, M. L.; Liu, Y.; Deng, S.-X.; Xie, Y.; Gong, G.; Aulner, N.; Többen, U.; Myers, K.; Chung, K.; Anderson, M.; Vidovic, D.; Schurer, S.; Branden, L.; Yamamoto, A.; Landry, D. W. Potent inhibitors of Huntingtin protein aggregation in a cell-based assay. *Bioorg. Med. Chem. Lett.* **2009**, *19*, 1715–1717.

(46) Ding, P.; Helquist, P.; Miller, M. J. Design and synthesis of a siderophore conjugate as a potent PSMA inhibitor and potential diagnostic agent for prostate cancer. *Bioorg. Med. Chem.* **2008**, *16*, 1648–1657.

(47) Blat, D.; Weiner, L.; Youdim, M. B. H.; Fridkin, M. A novel iron-chelating derivative of the neuroprotective peptide NAPVSIPQ shows superior antioxidant and antineurodegenerative capabilities. *J. Med. Chem.* **2008**, *51*, 126–134.

(48) Miranda, C. L.; Stevens, J. F.; Ivanov, V.; McCall, M.; Frei, B.; Deinzer, M. L.; Buhler, D. R. Antioxidant and prooxidant actions of prenylated and nonprenylated chalcones and flavanones in vitro. *J. Agric. Food Chem.* **2000**, *48*, 3876–3884.

(49) Rodriguez, R. J.; Miranda, C. L.; Stevens, J. F.; Deinzer, M. L.; Buhler, D. R. Influence of prenylated and non-prenylated flavonoids on liver microsomal lipid peroxidation and oxidative injury in rat hepatocytes. *Food Chem. Toxicol.* **2001**, *39*, 437–445.

(50) Li, C.-Y.; Wang, Y.; Hu, M.-K. Allylmagnolol, a novel magnolol derivative as potent antioxidant. *Bioorg. Med. Chem.* **2003**, *17*, 3665–3671.

(51) Seyedi, S. M.; Jafari, Z.; Attaran, N.; Sadeghian, H.; Saberi, M. R.; Riazi, M. M. Design, synthesis and SAR studies of 4-allyoxyaniline amides as potent 15-lipoxygensae inhibitors. *Bioorg. Med. Chem.* **2009**, *17*, 1614–1622.

(52) Sawada, G. A.; Williams, L. R.; Lutzke, B. S.; Raub, T. J. Novel, highly lipophilic antioxidants readily diffuse across the blood-brain barrier and access intracellular sites. *J. Pharmacol. Exp. Ther.* **1999**, *288*, 1327–1333.

(53) Youdim, K. A.; Dobbie, M. S.; Kuhnle, G.; Proteggente, A. R.; Abbott, N. J.; Rice-Evans, C. J. Interaction between flavonoids and the blood−brain barrier: in vitro studies. *Neurochemistry* **2003**, *85*, 180–192.

(54) Braughler, J. M.; Duncan, L. A.; Chase, R. L. The involvement of iron in lipid peroxidation. Importance of ferric to ferrous ratios in initiation. *J. Biol. Chem.* **1986**, *261*, 10282–10289.

(55) Maynard, C. J.; Bush, A. I.; Masters, C. L.; Cappai, R.; Li, Q.-X. Metals and amyloid-β in Alzheimer's disease. *Int. J. Exp. Pathol.* **2005**, *86*, 147–159.

(56) Jayasena, T.; Grant, R. S.; Keerthisingle, N.; Solaja, I.; Smythe, G. A. Membrane permeability of redox active metal chelators: an important element in reducing hydroxyl radical induced NAD^+ depletion in neuronal cells. *Neurosci. Res.* **2007**, *57*, 454–461.

(57) Huang, X.; Moir, R. T.; Tanzi, R. E.; Bush, A. I.; Rogers, J. T. Redox-active metals, oxidative stress, and Alzheimer's disease pathology. *Ann. N.Y. Acad. Sci.* **2004**, *1012*, 153–163.

(58) Cuajungco, M. P.; Fagét, K. Y.; Huang, X.; Tanzi, R. E.; Bush, A. I. Metal chelation as a potential therapy for Alzheimer's disease. *Ann. N.Y. Acad. Sci.* **2000**, *920*, 292–304.

(59) Hider, R. C.; Ma, Y.; Molina-Holgado, F.; Gaeta, A.; Roy, S. Iron chelation as a potential therapy for neurodegenerative disease. *Biochem. Soc. Trans.* **2008**, *36*, 1304–1308.

(60) Beetsch, J. W.; Park, T. S.; Dugan, L. L.; Shah, A. R.; Gidday, J. M. Xanthine oxidase-derived superoxide causes reoxygenation injury of ischemic cerebral endothelial cells. *Brain Res.* **1998**, *786*, 89–95.

(61) Abramor, A. Y.; Scorziello, A.; Duchen, M. R. Three distinct mechanisms generate oxygen free radicals in neurons and contribute to cell death during anoxia and reoxygenation. *J. Neurosci.* **2007**, *27*, 1129–1138.
(62) Qin, C. X.; Chen, X.; Hughes, R. A.; Williams, S. J.; Woodman, O. L. Understanding the cardioprotective effects of flavonoids: discovery of relaxant flavonols without antioxidant activity. *J. Med. Chem.* **2008**, *51*, 1874–1884.
(63) Gong, J.; Weng, L.; Wang, F.; Feng, Y.; Zhou, C.; Li, H.; Wu, Y.; Hao, X.; Wu, X.; Bai, H.; Stöckigt, J.; Zhao, Y. Synthesis and antioxidant properties of novel silybin analogues. *Chin. Chem. Lett.* **2006**, *17*, 465–468.
(64) Hansel, R.; Schulz, J.; Pelter, A. Structure of silybin. II. Synthesis of dehydrosilybin pentamethyl ether and related compounds. *Chem. Ber.* **1975**, *108*, 1482–1501.
(65) Merlini, L.; Zanarotti, A.; Pelter, A.; Rochefort, M. P.; Hansel, R. Benzodioxanes by oxidative phenol coupling, synthesis of silybin. *J. Chem. Soc., Perkin Trans 1* **1980**, 775–778.
(66) Tanaka, H.; Shibata, M.; Ohira, K.; Ito, K. Total synthesis of (±)-silybin, and antihepatotoxic flavonolignan. *Chem. Pharm. Bull.* **1985**, *33*, 1419–1423.
(67) Li, S.; Wu, Y.; Ji, Z. Total synthesis of 2*R*,3*R*-(+)-silybin as an antihepatoxic natural product. *Chin. J. Med. Chem.* **1997**, *7*, 107–111.
(68) Zou, H.; Dong, S.; Zhou, C.; Hu, L.; Wu, Y.; Li, H.; Gong, J.; Sun, L.; Wu, X.; Bai, H.; Fan, B.; Hao, X.; Stöckigt, J.; Zhao, Y. Design, synthesis and SAR analysis of cytotoxic sinapyl alcohol derivatives. *Bioorg. Med. Chem.* **2006**, *14*, 2060–2071.
(69) Lee, D. Y.-W.; Liu, Y. Molecular structure and stereochemistry of silybin A, silybin B, isosilybin A, and isosilybin B, isolated from *Silybum marianum* (milk thistle). *J. Nat. Prod.* **2003**, *66*, 1171–1174.
(70) Gong, J.; Huang, K.; Wang, F.; Yang, L.; Feng, Y.; Li, H.; Li, X.; Zeng, S.; Wu, X.; Stöckigt, J.; Zhao, Y.; Qu, J. Preparation of two sets of 5,6,7-trioxygenated dihydroflavonol derivatives as free radical scavengers and neuronal cell protectors to oxidative damage. *Bioorg. Med. Chem.* **2009**, *17*, 3414–3425.
(71) Kónya, K.; Varga, Zs.; Antus, S. Antioxidant properties of 8.O.4′-neolignans. *Phytomedicine* **2001**, *8*, 454–459.
(72) Czompa, A.; Dinya, Z.; Antus, S.; Varga, Zs. Synthesis and antioxidant activity of flavonoid derivatives containing a 1,4-benzodioxane moiety. *Arch. Pharm. Pharm. Med. Chem.* **2000**, *333*, 175–180.
(73) Wilkinson, B. L.; Landreth, G. E. The microglial NADPH oxidase complex as a source of oxidative stress in Alzheimer's disease. *J. Neuroinflammation* **2006**, *3*, 30.
(74) Joubert, E.; Winterton, P.; Britz, T. J.; Ferreira, D. Superoxide anion and α,α-diphenyl-β-picrylhydrazyl radical scavenging capacity of rooibos (*Aspalathus linearis*) aqueous extracts, crude phenolic fractions, tannin and flavonoids. *Food Res. Int.* **2004**, *37*, 133–138.
(75) Nordberg, J.; Arner, E. S. J. Reactive oxygen species, antioxidans, and the mammalian thioredoxin system. *Free Radical Biol. Med.* **2001**, *31*, 1287–1312.
(76) Mukherjee, S.; Kumar, V.; Prasad, A. K.; Raj, H. G.; Bracke, M. E.; Olsen, C. E.; Jain, S. C.; Parmar, V. S. Synthetic and biological activity evaluation studies on novel 1,3-diarylpropenones. *Bioorg. Med. Chem.* **2001**, *9*, 337–345.
(77) van Acker, F. A.; Hageman, J. A.; Hanen, G. R.; van Der Vijgh, W. J.; Bast, A.; Menge, W. M. Synthesis of novel 3,7-substituted-2-(3′,4′-dihydroxyphenyl)flavones with improved antioxidant activity. *J. Med. Chem.* **2000**, *43*, 3752–3760.
(78) Bennett, C. J.; Caldwell, S. T.; McPhail, D. B.; Morrice, P. C.; Duthie, G. G.; Hartley, R. C. Potential therapeutic antioxidants that combine the radical scavenging ability of myricetin and the lipophilic chain of vitamin E to effectively inhibit microsomal lipid peroxidation. *Bioorg. Med. Chem.* **2004**, *12*, 2079–2098.
(79) Yang, B.; Kotani, A.; Arai, K.; Kusu, F. Estimation of the antioxidant activities of flavonoids from their oxidation potentials. *Anal. Sci.* **2001**, *17*, 599–604.
(80) Takahashi, K.; Kunishiro, K.; Kasai, M.; Miike, T.; Kurahashi, K.; Shirahase, H. Relationships between lipophilicity and biological activities in a series of indoline-based anti-oxidative acyl-CoA:cholesterol acyltransferase (ACAT) inhibitors. *Arzneimittelforschung* **2008**, *58*, 666–672.
(81) Koufaki, M.; Calogeropoulou, T.; Detsi, A.; Roditis, A.; Kourounakis, A. P.; Papazafiri, P.; Tsiakitzis, K.; Gaitanaki, C.; Beis, I.; Kourounakis, P. N. Novel potent inhibitors of lipid peroxidation with protective effects against reperfusion arrhythmias. *J. Med. Chem.* **2001**, *44*, 4300–4303.
(82) Molochkina, E. M; Zorina, O. M.; Fatkullina, L. D.; Goloschapov, A. N.; Burlakova, E. B. H_2O_2 modifies membrane structure and activity of acetylcholinesterase. *Chem.−Biol. Interact.* **2005**, *157−158*, 401–404.
(83) Coyle, J. T.; Puttfarcken, P. Oxidative stress, glutamate, and neurodegenerative disorders. *Science* **1993**, *262*, 689–695.
(84) Leopoldini, M.; Russo, N.; Chiodo, S.; Toscano, M. Iron chelation by the powerful antioxidant flavonoid quercetin. *J. Agric. Food Chem.* **2006**, *54*, 6343–6351.
(85) Borsari, M.; Gabbi, C.; Ghelfi, F.; Grandi, R.; Saladini, M.; Severi, S.; Borella, F. Silybin, a new iron-chelating agent. *J. Inorg. Biochem.* **2001**, *85*, 123–129.
(86) Bouwkamp, M. W.; Bowman, A. C.; Lobkovsky, E.; Chirik, P. J. Iron-catalyzed [2π + 2π] cycloaddition of α,ω-dienes: the importance of redox-active supporting ligands. *J. Am. Chem. Soc.* **2006**, *128*, 13340–13341.
(87) Yermolaieva, O.; Xu, R.; Schinstock, C.; Brot, N.; Weissbach, H.; Heinemann, S.; Hoshi, T. Methionine sulfoxide reductase A protects neuronal cells against brief hypoxia/reoxygenation. *Proc. Natl. Acad. Sci. U.S.A.* **2004**, *101*, 1159–1164.
(88) van Roon-Mom, W. M. C.; Pepers, B. A.; 't Hoen, P. A. C.; Verwijmeren, C. A. C. M.; den Dunnen, J. T.; Dorsman, J. C.; van Ommen, G. B. Mutant huntington activates Nrf2-responsive genes and impairs dopamine synthesis in a PC12 model of Huntington's disease. *BMC Mol. Biol.* **2008**, *9*, 84.
(89) Saito, Y.; Nishio, K.; Ogawa, Y.; Kinumi, T.; Yoshida, Y.; Masuo, Y.; Niki, E. Molecular mechanisms of 6-hydroxydopamine-induced cytotoxicity in PC12 cells: involvement of hydrogen peroxide-dependent and -independent action. *Free Radical Biol. Med.* **2007**, *42*, 675–685.
(90) Gelinas, S.; Bureau, G.; Valastro, B.; Massicotte, G.; Cicchetti, F.; Chiasson, K.; Gagne, B.; Blanchet, J.; Martinoli, M.-G. Alpha and beta estradiol protect neuronal but not native PC12 cells from paraquat-induced oxidative stress. *Neurotox. Res.* **2004**, *6*, 141–148.
(91) van de Waterbeemd, H.; Kansy, M. Hydrogen-bonding capacity and brain penetration. *Chimia* **1992**, *46*, 299–305.
(92) Cao, G.; Sofic, E.; Prior, R. L. Antioxidant and prooxidant behavior of flavonoids: structure−activity relationships. *Free Radical. Biol. Med.* **1997**, *22*, 749–760.
(93) Arora, A.; Nair, M. G.; Strasburg, G. M. Structure−activity relationships for antioxidant activities of a series of flavonoids in a liposomal system. *Free Radical Biol. Med.* **1998**, *24*, 1355–1363.
(94) Bors, W.; Michel, C.; Stettmaier, K. Antioxidant effects of flavonoids. *Biofactors* **1997**, *6*, 399–402.
(95) Ochiai, T.; Takenaka, Y.; Kuramoto, Y.; Kasuya, M.; Fukuda, K.; Kimura, M.; Shimeno, H.; Misasi, R.; Hiraiwa, M.; Soeda, S. Molecular mechanism for neuroprotective effect of prosaposin against oxidative stress: its regulation of dimeric transcription factor formation. *Biochim. Biophys. Acta* **2008**, *1780*, 1441–1447.
(96) Li, R. C.; Pouranfar, F.; Lee, S. K.; Morris, M. W.; Wang, Y.; Gozal, D. Neuroglobin protects PC12 cells against beta-amyloid-induced cell injury. *Neurobiol. Aging* **2008**, *29*, 1815–1822.
(97) Schroeter, H.; Spencer, J. P.; Rice-Evans, C.; Williams, R. J. Flavonoids protect neurons from oxidized low-density-lipoprotein-induced apoptosis involving c-Jun N-terminal kinase (JNK), c-Jun and caspase-3. *Biochem. J.* **2001**, *358*, 547–557.
(98) Williams, R. J.; Spencer, J. P.; Rice-Evans, C. Flavonoids: antioxidants or signalling molecules? *Free Radical Biol. Med.* **2004** *36*, 838–849.
(99) Spencer, J. P. E. The interactions of flavonoids within neuronal signalling pathways. *Gen. Nutr.* **2007**, *2*, 257–273.
(100) Fatokuna, A. A.; Stonea, T. W.; Smith, R. A. Hydrogen peroxide mediates damage by xanthine and xanthine oxidase in cerebellar granule neuronal cultures. *Neurosci. Lett.* **2007**, *416*, 34–38.
(101) Lin, C. M.; Chen, C. S.; Chen, C. T.; Liang, Y. C.; Lin, J. K. Molecular modeling of flavonoids that inhibits xanthine oxidase. *Biochem. Biophys. Res. Commun.* **2002**, *294*, 167–172.
(102) Van Hoorn, D. E.; Nijveldt, R. J.; Van Leeuwen, P. A.; Hofman, Z.; M'Rabet, L.; De Bont, D. B.; Van Norren, K. Accurate prediction of xanthine oxidase inhibition based on the structure of flavonoids. *Eur. J. Pharmacol.* **2002**, *451*, 111–118.
(103) Cos, P.; Ying, L.; Calomme, M.; Hu, J. P.; Cimanga, K.; Van Poel, B.; Pieters, L.; Vlietinck, A. J.; Vanden Berghe, D. Structure−activity relationship and classification of flavonoids as inhibitors of xanthine oxidase and superoxide scavengers. *J. Nat. Prod.* **1998**, *61*, 71–76.
(104) Takuma, K.; Baba, A.; Matsuda, T. Astrocyte apoptosis: implications for neuroprotection. *Prog. Neurobiol.* **2004**, *72*, 111–127.
(105) Blois, M. S. Antioxidant determinations by the use of a stable free radical. *Nature* **1958**, *181*, 1199–1200.

(106) Robak, J.; Gryglewski, R. J. Flavonoids are scavengers of superoxide anions. *Biochem. Pharmacol.* **1988**, *37*, 837–841.
(107) Janero, D. Malondialdehyde and thiobarbituric acid-reactivity as diagnostic indices of lipid peroxidation and peroxidative tissue injury. *Free Radical Biol. Med.* **1998**, *9*, 515–540.
(108) Armstrong, D.; Browne, R. The analysis of free radicals, lipid peroxidases, antioxidant enzymes and compounds related to oxidative stress as applied to the clinical chemistry laboratory. *Adv. Exp. Med. Biol.* **1994**, *366*, 43–58.
(109) Carter, P. Spectrophotometric det. of serum iron at the submicrogram level with a new reagent (Ferrozine). *Anal. Biochem.* **1971**, *40*, 450–458.
(110) Yang, L. X.; Zhang, L. J.; Huang, K. X.; Li, X. K.; Hu, L. H.; Wang, X. Y.; Stöckigt, J.; Zhao, Y. Antioxidant and neuroprotective effects of synthesized sintenin derivatives. *J. Enzyme Inhib. Med. Chem.* **2009**, *24*, 425–431.
(111) Wang, F.; Yang, L.; Huang, K.; Li, X.; Hao, X.; Stöckigt, J.; Zhao, Y. Preparation of ferulic acid derivatives and evaluation of their xanthine oxidase inhibition activity. *Nat. Prod. Res.* **2007**, *21*, 196–202.
(112) Majklc-Singh, N.; Bogarae, L.; Kalimanovska, V.; Jelie, Z.; Spasis, S. Spectrophtometric assay of xanthine oxidase with 2,2′-azino-di(3-ethylbenthiazoline-6-sulphonate) (ABTS) as chromogen. *Clin. Chim. Acta* **1987**, *162*, 29–36.